S-1952

FR-1952

Code 5520

[redacted] [redacted]

27 October 1942 DECLASSIFIED Report No. S-1952

NAVY DEPARTMENT

Report on

The Shock Produced by a Collapsing Cavity in Water

NAVAL RESEARCH LABORATORY
ANACOSTIA STATION
WASHINGTON, D. C.

Number of Pages: Text - 20 Plates - 20

Reported by: M. F. M. Osborne
M. F. M. Osborne, Contract Employee

Reviewed by: H. C. Hayes
Dr. H. C. Hayes, Principal Physicist, Superintendent Sound Division

Approved by: R J Walker
R. J. Walker, Commander U.S.N.

Distribution:
BuShips (2)
Cominch (Readiness) (2)
C.R. & D. (5)
BuOrd (re 6b) (2) 6b
NOL (2)
NDRC (3)
D. Taylor Model Basin (2)
British Central Sci. Office (5)
H.M. A/S E.E., Fairlie (2)
Fleet Sound School - Key West (1)
Fleet Sound School - San Diego (1)
USS SEMMES (1)
Radio & Sound Lab., San Diego (1)
Radio & Sound Lab., New London (1)
Files (10)

ABSTRACT

This report presents the results of an experimental study of the shock produced by a collapsing cavity in water. Such a study is significant for three fields of investigation: a) for noise analysis, since cavitation is an important cause of noise from the propellers of ships and from objects dragged through the water at high speeds; b) for underwater explosions, since these experiments reproduce in miniature the conditions which obtain shortly after the detonation of a mine; and c) for cavitation erosion and the water-hammer breakage of glass containers.

It is shown that cavitation shocks are recurrent or multiple, the time interval separating them depending primarily on the size of the cavity. Further, it is shown that the abruptness and violence of the shock, the total acoustic energy produced and its frequency distribution, are all highly dependent on the size of the residual air bubble around which the cavity collapses. The size of this bubble determines the degree of cushioning of the shock; hence the undesirable characteristics of the shock, as measured by noise production and mechanical destruction, are much diminished as the air bubble size increases, and the predominant frequency of the noise generated shifts to the lower frequencies. Quantitative relationships for these variables have been obtained as a function of cavity size (or energy content of the blow) and air bubble size.

[redacted]

TABLE OF CONTENTS

PLATES

I. INTRODUCTION

1. A study of the collapse of a cavity in water was originally undertaken for the purposes of noise analysis, with particular reference to the noise produced around propellers and in the turbulent wake of an underwater sound projector of echo-ranging equipment. Since very little quantitative data on the nature of the acoustic shocks so produced were available, it seemed desirable to investigate them under controlled conditions, so that their properties might be better understood and, if possible, a method for their suppression developed. Such an investigation has been conducted. In the following paragraphs the experiments are described and the results are presented.

2. The results of this investigation are also pertinent to the discussion of the oscillation of the gas bubble around an exploded mine, and to the mechanical destruction which cavitation shocks can produce.

II. APPARATUS

3. The experimental apparatus consisted of a vessel containing a constant amount of water. The volume of this vessel could be varied by means of a brass sylphon bellows in one wall. Thus a cavity, the formation of which required a known amount of energy, and which contained a known volume of air, could be made to collapse in the vessel. The resulting shock was picked up by a small quartz microphone, mounted in water either inside or outside the vessel. This shock, amplified and put on the screen of a cathode-ray oscillograph, was photographed on motion picture film with a revolving-drum camera.

4. The important part of the apparatus is illustrated in Plate 1. It consisted of a cylindrical glass or brass vessel, full of air-free water, and containing a quartz microphone. A stop-cock in the cylindrical wall permitted the introduction of water or a small air-bubble of known volume. In the case of the brass vessel, the upper end was a disc of 1/2" plate glass so that the interior could be easily observed. The ends of the cylindrical vessel were made water tight by rubber gaskets. Two brass plates and four long bolts clamped the cylinder and its two ends together, and kept the gasketed assembly under compression.

5. The sylphon bellows and the outlet for the microphone were at the lower end of the cylinder. The armature of an electromagnet was attached to the sylphon bellows. When a picture was taken, the armature was released by the same switch which opened

[redacted]

which opened the shutter of the camera, thus synchronizing shock and photograph. The sylphon bellows and armature were surrounded by a metal cylinder which served to support the electromagnet and to keep water away from the sylphon bellows and armature when the entire assembly was immersed in a big tank (sylphon bellows end down). The motion of the sylphon bellows and armature was thus unimpeded.

6. Except when the two were actually in contact, the electromagnet was electrically insulated from the armature. This made it possible to record on the photographic film the starting time of collapse as determined by the time when the electromagnet let go of the armature.

7. The microphone consisted of 4 X-cut quartz crystals, each 12 mm by 12 mm by 2 mm, connected in parallel. These were so mounted that the faces perpendicular to the Y axis were sensitive faces. They were enclosed in a brass drum-shaped holder, the faces of the drum being German silver sheets 0.002" thick and 12 mm apart, and the sensitive faces of the crystals being just behind the drum faces. Castor oil provided mechanical contact between the inner faces of the drum and the sensitive faces of the crystals. The leakage resistance of the microphone was so low (23,000 ohms), and therefore its time constant (=RC) so small, that its voltage response was proportional to the time derivative of the impressed pressure wave. Hence the oscillograms represent the variations of $\partial p/\partial t$ within the limitations discussed in the Appendix. Calibration of the microphone-amplifier system gave a curve of response which increased linearly with frequency, in agreement with this. See Plate 2.

8. A General Radio 714-A Voltage Amplifier amplified the transient from the microphone, and put it on the horizontal plates of a General Radio 687 BS5 Electron Oscillograph. The camera was a General Radio 651A and 651A3 1 Camera Assembly. The camera was not used in the normal way. Instead, a single turn of film was put on the sprocket wheel, which was driven by a belt from the take-up, rather than by the drive motor. In this way, film speeds up to 80 ft. per sec. were attainable. The film used was Agfa Super-Pan Supreme.

9. For purposes of timing and voltage calibration, a standard 1000 cycle voltage was put through a microvolter and applied to the input terminals of the amplifier. This was switched in just after the transient. The rest position of the oscillograph spot was at the same time shifted by means of B batteries between the ground side of the amplifier and the low potential side of the oscillograph. Thus, on the films the transient appears in the center of the film, the standard signal at the edge. For some photographs this battery circuit was broken when the armature separated from the electromagnet. This is shown by a jump of the oscillograph trace towards the middle of the film and indicates the instant

at which collapse began.

10. For film speeds greater than 30 ft. per sec. the drum revolved more than once while the shutter was still open. To avoid overrunning of the spot trace on the film, a charged condenser and resistance in parallel were connected in series with the B batteries. This RC circuit was closed when the relay on the electromagnet circuit opened. The spot then shifted in the course of the exposure giving a helical trace on the single turn of film.

III. EXPERIMENTAL PROCEDURE

11. When tap water was put directly into the vessel, and the sylphon bellows expanded, a fine froth of bubbles formed throughout the liquid, due to the reduced pressure. Therefore, the water in the vessel had to be first freed of air, since otherwise it was impossible to control the size of the air bubble around which the cavity collapsed. This was done by boiling the water in the vessel for a half hour or more, the steam escaping through the stop-cock in the side. It was then allowed to cool and draw back water which had also been boiled over the same interval. Any residual bubble could then be shaken out.

12. The pinch-cock at the outer end of the rubber tube, beyond the glass stop-cock, was to hold a water reservoir in the tube for cooling shrinkage or other losses. See Plate 1. The pinch-cock nearest the vessel prevented the rubber tube from collapsing when the sylphon was expanded in order to form a cavity in the vessel.

13. With such preparation, when the armature on the bellows was first pulled down with the fingers, a distinct initial resistance was felt, representing the slight tension which the water could sustain. This resistance suddenly gave way with the formation of the cavity, the force thereafter being very nearly a constant (atmospheric pressure). If the sylphon bellows were released slowly, a minute bubble (diameter less than 0.3 mm for freshly boiled water) was to be seen at the site of the cavity. It was released either from the water or from the adsorbed gasses in the metal or glass of the vessel. If the armature were again pulled down, the initial resistance was no longer felt, the force increasing rapidly but continuously to a nearly constant value. See Plate 3. The bubble likewise increased continuously in size. If one waited until the small bubble redissolved, the initial resistance could again be felt.

14. This small bubble represented the lower limit which could be reached with this apparatus. For water which in time dissolved more air, either through leaks or from larger air bubbles introduced deliberately through the stop-cock, this minimum bubble could be 2 mm in diameter. Hence no observation could be made with a smaller air bubble without reboiling.

15. It is believed that air bubbles about 1 mm in diameter or less are characteristic of those which are present in true cavitation shocks, where the cavity forms and collapses in a time too short for much air to dissolve out due to the decreased pressure. Baker (1)

has described the water-hammer breakage of glass containers, essentially a cavitation phenomenon. He was able to burst glass jars partially filled with liquid by violently accelerating them. The cavity formed when the liquid was "left behind" burst the jar on collapsing. It was found in the present experiment that the glass vessel, made from a heavy pyrex bottle with walls 1/8" to 3/16" thick, burst with depressing regularity when the air bubbles were about 1 mm in diameter or less, depending somewhat on the amount of energy released in the blow. It was for this reason that the brass vessel with the 1/2" plate glass end was built. This was better able to withstand the shock.

16. In the observation of a cavitation shock, the following procedure was adopted. The size of the air bubble and the distance through which the armature moved were measured, thus determining the mechanical energy to be released. The armature was then pulled back to the face of the electromagnet, which was just strong enough to hold it. With the drum and film revolving at a steady rate, the camera shutter was snapped, and simultaneously the electromagnet let go. The oscillograph spot was then shifted and a standard signal from the microvolter photographed. Finally, the size of the air bubble was remeasured, though the pieces of it had to be shaken together again with the bellows slightly expanded by hand.

17. The measured sizes of the air bubble, before and after the shock, agreed fairly well even for small bubbles, provided:

a) the measurement was made immediately after the shock, and

b) the water had not much air dissolved in it, or the bubbles were large (greater than 25 cu.mm).

If the water had considerable air dissolved in it, additional air which had dissolved out while the bellows was expanded made the second volume measure somewhat uncertain, but with care and judgment satisfactory agreement was obtainable.

18. The volume was computed on the assumption that the bubble was spherical if small, or ellipsoidal with measured axis ratio if flattened. The volume of larger bubbles was measured in the cylindrical tube near the glass stop-cock. See Plate I.

19. Observations were made under the following conditions:-

a) Brass vessel immersed in water. Position vertical. Microphone inside and outside. Differences for the microphone outside are relatively small, since the same type of shock acts on the inside.

b) Brass vessel in air. Position vertical and horizontal. Microphone inside. This was a run at one energy of blow only, to determine the effect of the shape of the cavity. In the vertical position, the cavity was wedge shaped, as the section of an orange. In a

horizontal position, the cavity had the form of a long thin slab the cross section of which was a segment of a circle.

c) Glass vessel in air. Position vertical. Microphone inside. This series was taken to test the effect of vessel material, and to establish effects poorly determined by previous measures. These data are the most homogeneous and complete over the range covered. The cavity was crescent shaped, owing to the bulging upward of the bottom of the bottle from which the vessel was made. A series of oscillograms illustrating these cases are given in Plates 16, 17, 18, 19, and 20. They are arranged in order of decreasing bubble size.

20. From these photographs the following measurements were made with a Hilger travelling microscope:

a) The scales in microsec./mm (x) and millivolts/mm (y).

b) The time of rise of the first peak, or the interval from a point where the deflection was first appreciable, to the first "principal" peak. The first point was naturally somewhat indeterminate, the initial rise being rather gradual. It is estimated, however, that the deflection became appreciable at about 1% of the maximum, if one takes 1/4 of the trace width as the least appreciable deflection. The width of the trace was about 0.12 mm, and the maximum deflection was usually between 2 and 4 mm on the film.

c) The time interval between 1/6 maximum deflection and the maximum. This was adopted as a fair criterion of the time over which most of the initial rise took place.

d) The height of the first maximum in millivolts. The choice of the first 'principal' maximum was usually clear cut, even though minor crepitations often immediately preceded it. The first principal maximum was always one of the highest - though not necessarily the highest, as a glance at the oscillograms will show. These measurements were taken only in cases where the microphone was inside.

e) The total time of collapse, from the instant of release of the armature to first peak. These were made only for the glass vessel in air.

f) The time interval between the first and second big shock. Where shocks of radically different type appeared, the second shock of the same type as the first was chosen for this measurement - e.g., see No. 1, Plate 19. Multiple shocks were least common for cavities of low energy and small air bubbles. In general, however, the presence of more than one shock was the rule rather than the exception.

g) The ratio of the amplitude of the second shock to that of the first.

h) Measures of the relative intensities of the characteristic vibrations present. Three distinct characteristic vibrations are observable in the oscillograms, of periods T_1=5000 - 10,000 microseconds, T_2=410 - 530 microseconds, and T_3= 20 microseconds.

An attempt was made to determine the initial rms pressure represented in these oscillations. The average initial amplitude in millivolts of these vibrations was estimated for two groups of data (glass vessel in air, brass vessel in water) for which approximately the same total energy was released in the shock.

21. The above measurements, determining the nature of the shock, are considered as functions of the independent variables V and E. V is the volume of the air bubble in cu mm, and E is the energy content of the shock as determined from the integrated force function of the bellows. If E is in ergs x 10^6, E is also approximately the size of the cavity, in cu cm.

22. The microphone-amplifier system was calibrated by comparison with standard microphones calibrated by the Bell Telephone Laboratories. For the low frequencies (less than 1000 cps) an electromagnetic sound source (3) was used; for the high, a Rochelle salt projector. The microphone was held edgewise with respect to the sound source, the same orientation it had relative to the shock. In Figure 2 the calibration of the system is given as if for no gain, since the standard microphone was connected to the input of an amplifier, and appropriate corrections due to the amplifier and its input impedance were applied.

23. The sign of the deflection of the oscillograph spot for a condensation wave was determined by photographing the transient due to tapping on a pail of water, the microphone being in the pail. For various orientations of the microphone the direction of initial deflection was the same, and indicated that the initial wave from the cavitation shock, inside and outside the vessel, was one of condensation, or the same as in the case of tapping on the pail.

24. An upper limit to the energy expended in pulling the armature from the electromagnet was determined by measuring the force-distance function for the armature. This was done by measuring the holding force for various thicknesses of paper between the armature and pole face. The work expended was found to be negligible compared to that of pulling the bellows.

IV. DISCUSSION

25. The discussion will be divided into three parts:

(A) A general description of the shocks.
(B) A discussion of the graphical results.
(C) A discussion of the extent to which the observations can be represented by theory.

(A) General Description of the Shocks

26. To the ear there was a marked difference between those shocks with an appreciable air bubble (more than 10 cu mm) and those with a small one (1 cu mm). In the first case the sound was a dull thud, in the latter a sharp click or clank.

27. Examination of the oscillograms also shows a marked change in their characteristics with diminishing size of the air bubble. For air bubbles with volumes 100 to 500 cu mm, the trace is initially a series of single waves, (see sketch), which after 2 or 3 cycles merge into a simple sinusoid. See Plate 16, No.2. The period is 5000 - 10000 microseconds, essentially the same as the interval between shocks. This is an underlying structure which persists even to the smallest bubble, and measurements indicate that its amplitude in millivolts actually increases slightly with diminishing air bubble size. See Plates 14 and 15. It is relatively less apparent in the shocks with smaller air bubbles, since other larger structures of periods, T_1 and T_3, appear and may mask it. Since the gain of the amplifier was cut down for the smaller bubbles, this oscillation appears to become negligible in this case.

28. For air bubbles 10 - 150 cu mm in volume, the second principal mode becomes prominent, $T_2 \approx$ 410 μsecs for the glass vessel, and 530 microseconds for the brass one. For the same size air bubble the higher frequency modes become more pronounced with increasing energy, as is to be expected from the fact that the time of rise is less. (See paragraph 33).

29. For air bubbles 10 cu mm in volume the third mode of oscillation appears. For these bubbles the clanking sound is noticeable. T_3 is probably a normal mode determined primarily by the shape of the vessel, since its wave length in water is comparable to the linear dimensions of the vessel. The other two are probably mechanical, the longer one being associated with the inertia of the water, atmospheric pressure, and the low stiffness factor of the sylphon bellows.

30. In view of the statement that deflections in the oscillograms are proportional to $\partial p/\partial t$, the choice of the first peak, as A, of sketch 1 for example, giving the end of collapse needs some justification, especially for the larger air bubbles.

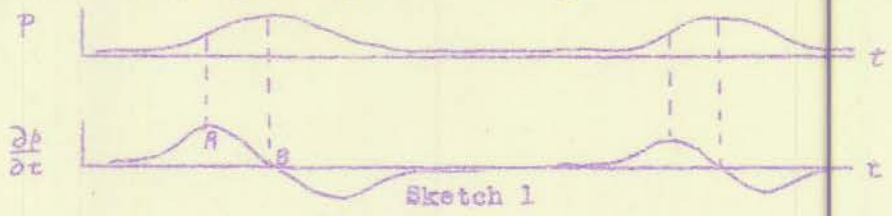

Sketch 1

It would seem more correct to choose the point B as the end of collapse. Such a choice would seriously modify the measured length of time for collapse. Nevertheless, it is believed that the structure of the sketch is a characteristic of the vessel rather than of the shock itself, and that the point A gives a better determination of the end of collapse than B. The structure persists, as mentioned before, throughout all the shocks, and if the point B were chosen as the end of collapse for the larger air bubbles, it would have to be used for all of them, out of consistency. However, the disturbance, as is obvious from the oscillograms, is initiated at the instant A, or first peak. By B a considerable damping of the higher modes of oscillation has already taken place. For example, see Plate 16, Nos. 13, 14 and Plate 17 Nos. 1, 2, 3, and 4. Therefore, it seems more reasonable to pick the end of collapse at the time when the disturbance evidently begins, at the first peak, A.

31. Another characteristic feature of these shocks is that they are repeated, the interval depending, as will be shown, on the size of the cavity. There is, moreover, a sort of double multiplicity. Between the principal shocks, which represent the oscillation of the cavity, there are often little shocks, always of high frequency components regardless of the type of the principal shocks. See, for example, Plate 17, Nos. 2 and 3. They probably represent cavitation at other parts of the vessel than the location of the air bubble.

32. It is interesting that repeated shocks appear even for the very smallest air bubbles. For such bubbles the compressibility of the water becomes important although the gas pressure is still negligible compared to the hydostatic pressure. See paragraph 44 and Appendix. Thus for the very smallest air bubbles one would expect the presence of gas in the cavity to have little effect on the nature of the shock. That oscillations or multiple shocks still occur under these conditions bears out the expectation of a previous investigation. (2). The formation of repeated shocks is probably favored by the fact that the collapse takes place at the upper end of a closed vessel, so that gravity and pressure act on the fluid in the same direction in reforming the cavity.

(B) Graphical Analysis

33. The time of rise of the first maximum from

[redacted]

$$\frac{\partial p}{\partial \tau} \simeq \frac{1}{100}\left(\frac{\partial p}{\partial t}\right)_{MAX} \quad \text{to} \quad \frac{\partial p}{\partial t} = \left(\frac{\partial p}{\partial t}\right)_{MAX}$$

and the time interval from

$$\frac{\partial p}{\partial \tau} = \frac{1}{5}\left(\frac{\partial p}{\partial \tau}\right)_{MAX} \quad \text{to} \quad \frac{\partial p}{\partial \tau} = \left(\frac{\partial p}{\partial \tau}\right)_{MAX}$$

are plotted in Plates 4, 5, 6, 7 for the cases there indicated. The convergence of the two curves is indicative of decreasing "abruptness" with increasing volume of air bubble. For the times for the last 4/5 of the shock there is a barely perceptible shift of the curves from one value of E (= energy released in shock) to the next. It is too uncertain to show in the total times of rise. By taking the intercepts of curves of different E with lines of constant bubble size, and plotting logarithmically, the exponential dependance on E can be obtained. The curves are sufficiently determinate to do this for bubble sizes V = 50 cu mm to V = 500 cu mm, and give the time for last 4/5 of peak =

$$C_1 E^{-0.321} V^{+0.555} = C_1 E^{+0.234} \left\{\frac{V}{E}\right\}^{+0.555}$$

for the glass vessel in air. For the brass vessel in water this time is

$$C_2 E^{-0.432} V^{+0.452} = C_2 E^{+0.020} \left\{\frac{V}{E}\right\}^{+0.452}$$

For some purposes the second form of the above formulae is useful, since, when the quantity V/E is constant, we can consider, by analogy to the detonation of a mine, that the cavities are produced by "explosives" of the same "chemical composition". In this form the importance of the relative size of the air bubble $\left\{\frac{V}{E}\right\}$ is emphasized, since the exponent of E alone is small.

34. The plots of the total time of collapse (given by the instant of release of armature and point A of the structure in Sketch 1 of paragraph 30) are given in Plates 8 and 9. Expressing by E cu mm, the equivalent volume in cu mm of a cavity whose production required E ergs, (using $p = 10^6$ dynes/cm^2), it will be observed that when the ratio V/E cu mm is less than a certain value $\left\{\frac{V}{E}_{\text{cu mm}} \simeq -0.005\right\}$ the time of collapse becomes almost independent of the air bubble size. This is to be expected when the gas pressure is comparable to the hydrostatic pressure over a time short compared to the total time of collapse. It will be shown later in Section C that the times of collapse computed under this assumption will be in agreement with experiment.

35. The time of collapse as a function of energy and the time interval between shocks are plotted on Plate 10, using only those data where $V/E_{\text{cu mm}} \leq 0.005$; i.e. where the approximation

neglecting the gas pressure is valid. It will be observed that the time interval between shocks is approximately twice the total time of collapse. This strengthens the conclusion that the successive shocks are actually the results of the oscillation of the cavity. Moreover the slope indicates that the period varies approximately as $E^{1/3}$, again in agreement with the theory for oscillations in an infinite medium (2). The validity of applying the infinite medium theory to a vessel of finite dimensions will be discussed in Section C. The two curves are not quite parallel, probably because the restoring force of the bellows was not quite constant.

36. The plots of the initial amplitudes as functions of energy and bubble size, are given in Plates 11 and 12 for the case of the brass vessel immersed in water, and the glass vessel in air. As before, by taking the intercepts of the different energy curves with lines of constant bubble size, and plotting logarithmically, the dependence on E can be obtained. The results are:

Glass vessel in air $\left(\frac{\partial p}{\partial t}\right)_{max} \propto$ Amplitude $= C_3 E^{+0.942} V^{-0.456} = C_3 E^{+0.936} \left(\frac{V}{E}\right)^{-0.456}$

Brass vessel in water $\left(\frac{\partial p}{\partial t}\right)_{max} \propto$ Amplitude $= C_4 E^{+0.942} V^{-0.437} = C_4 E^{+0.505} \left(\frac{V}{E}\right)^{-0.937}$

37. In Plates 6 and 13, the results obtained with the brass vessel in both vertical and horizontal positions in air are given. The results indicate that the amplitude and time to first maximum are, within the limits of experiment, independent of the shape of the cavity. However, for the horizontal position, in which the cavity was in the shape of a thin slab, the initial rise was more irregular than for the vertical position, as if the cavity did not collapse in one piece. See Plate 19.

38. For purposes of estimating the initial rms pressures of the noise produced by these shocks as a function of frequency, the average initial amplitudes of the three principal oscillations which appeared were measured, corrected by the microphone calibration curve, and plotted in Plates 14 and 15. As is evident from the graphs, the rms pressures of all three frequencies increase as the bubble size decreases. The increase is more pronounced for the higher frequencies. Also, for any given bubble size, there is more noise at low frequencies than at high. The data for Plate 15 were taken from a different run from that of Plates 4 and 12. This run is plotted in Plates 13 (lower curve) and 5, and seems to differ slightly from the other data for the glass vessel in air.

39. If the above data were converted to total energies by squaring the amplitudes and by taking into account the approximate length of train which each frequency produces, the above mentioned effects would be even more pronounced, since as is seen from the oscillograms, the high frequency noise damps out faster than the low.

40. The increase of high frequency noise for diminishing bubble size and the predominance of low frequency noise over high frequency in cavitation shocks, are facts to be expected from previous investigations. The first indicates that a sharp shock has more high frequency components than a dull one, e.g. tapping

on the vessel with a metal rod produced primarily T_3, and a wooden one produces primarily T_2. The second has been known from many observations on underwater noise, and is one reason for the use of the supersonic rather than the audio frequency range in underwater sound gear. Quantitatively, the data of this report are, of course, peculiar to the apparatus. Qualitatively, they may be expected to hold generally.

41. The ratio of the amplitude of the second shock to that of the first showed no marked correlation either with energy content or air bubble size. The mean was 0.55, the range from 0.3 to 1.2.

(C) Agreement of Observations with Theory

42. The formula for the total time of collapse (2) of a spherical cavity in an infinite medium is $T=1/2\ 1.135\ \rho^{1/2}\ p_\infty^{-5/6} E^{1/3}$. In the case of collapse in the presence of rigid boundaries, the time is somewhat longer, but the corrections are small when the distance to the boundary is large compared to the dimensions of the cavity. In the case of the collapse in a cylindrical vessel, we may approximate the conditions in either of two ways, as suggested in Sketch 2.

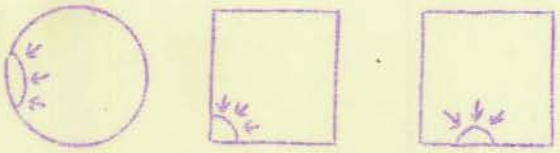

Sketch 2

APPROXIMATIONS

In case A, we replace the actual condition by a collapse in a rectangular trihedral angle. Then the formula for the infinite medium would be multiplied by 8, and by a small correction factor for the walls. In case B the collapse is represented as taking place in a rectangular dihedral. The formula for the infinite medium would be multiplied by 4, and a somewhat larger but still small correction factor for the disturbing boundaries would be used. Therefore, as a formula which is expected only to be correct in order of magnitude,

$$T \simeq 6 \times \tfrac{1}{2} \times 1.135\ \rho^{\frac{1}{2}}\ p_\infty^{-\frac{5}{6}}\ E^{\frac{1}{3}}$$

This is plotted in Plate 10 for $p_\infty = 10^6$ dynes/cm^2

The agreement is as good as would be expected without more refined consideration (such as increasing the pressure to allow for the stiffness of the sylphon), and shows that the neglect of compressibility and gas pressure effects in small air bubbles is justified in calculating the total time of collapse.

43. It does not seem possible to represent the observed variations of $\partial p/\partial t$ with the assumption of incompressibility, nor does it represent even a fair first approximation using a quasi-acoustic

[redacted]

theory. No satisfactory theory for collapse taking into account compressibility has been worked out. However, the incompressible theory can be used to verify the previous statement that for the smallest air bubbles, the gas pressure effects are negligible compared to the compressibility effects in the water. Compressibility effects are important when the velocity of collapse equals that of sound. Gas pressure is significant when it equals the hydrostatic pressure. It is therefore desired to calculate, on the basis of the incompressible theory, the value of $\frac{V}{E}_{\text{cu mm}}$ for which the velocity of collapse equals the velocity of sound at the same instant that the gas pressure equals the hydrostatic pressure. For values of V/E cu mm much smaller than this, one can expect the cavitation shock to be much the same as if no air at all were present.

44. It is shown in the Appendix II that this value of $\frac{V}{E}_{\text{cu mm}} = 5.5\times10^{-7}$ Thus for $E_{\text{cu mm}} = 13\times10^{3}$ cu mm. ($E = 13 \times 10^{6}$ ergs) $V = 0.0072$ cu mm. This is at the very lowest limit of observation. See Figure 20, No. 13.

45. One can also determine the value of $\frac{V}{E}_{\text{cu mm}}$ for which the maximum velocity of collapse equals the velocity of sound. (See Appendix II). This value is $V/E_{\text{cu mm}} = 2.8\times10^{-3}$. For example, $V=28$ cu mm for $E=10\times10^{6}$ ergs. This is well within the range of the experiments. For values of $V/E_{\text{cu mm}}$ much larger than this one would expect the incompressible approximation to be valid in describing the motion in detail. However, attempts so far have been unsuccessful in representing by theory the variation of $\partial p/\partial t$ or the time of rise with E or V. The disagreement may be attributed to the disturbing effect of the boundaries, turbulence and instability during collapse, a finite rate of condensation of the water vapor, or some other unknown reason.

V. CONCLUSIONS

46. Cavitation shocks are multiple, and the interval between shocks is predictable on the basis of theory.

47. The characteristics of the pressure wave produced by a cavitation shock are dependent on the size of the cavity, and especially on the air bubble it contains. The peak pressure derivative and the time of rise to its maximum are representable in the form $C\ E^{m}\gamma^{n}$. The characteristics of the wave are relatively less sensitive to the shape of the cavity, and for the two cases of this experiment, to the material of the walls against which the collapse takes place.

48. The noise generated decreases as the bubble size increases, the diminution being more pronounced for high frequency noise, and for all sizes of air bubbles more low frequency noise is present than high. The general effect of the air bubble is markedly to cushion the shock, and to mitigate its noise producing and destructive characteristics. This fact suggest the introduction of gas bubbles into water at points where the suppression of cavitation noise or erosion would be desirable.

49. The errors involved in the use of a time derivative microphone and imperfect amplifier can be estimated quite generally, and suggest a technique useful when the exact calibration of the microphone is difficult.

BIBLIOGRAPHY

(1) Baker, T. C. The Glass Industry 1941
Vol. 22, 430, 469, 521

(2) Herring, C. NDRC Report 6136 1941
Rep. No. C4SR20-010

(3) Ide, J. M. NRL Report No. S-1882 1942

[redacted]

APPENDIX I - Microphone Calibration

50. It has now to be shown that the microphone responds to the time derivative of the pressure wave. This can be shown quite generally when certain conditions are fulfilled, and may be useful in the interpretation of oscillograms from microphones whose direct calibration is not practicable. To do this consider the effect of impressing a unit, or step pressure wave on the microphone. Two types of disturbance are set up:

(a) Mechanical disturbances. If there are no large mechanical systems coupled to the crystals, these disturbances may be expected to die out in a time comparable to the time for the pressure wave to traverse the dimensions of the crystal a few times, since with each traversal a good part of the energy will be reradiated into the water.

(b) Electrical disturbances. These die out in a time determined by the duration of the mechanical disturbance, and by the capacitance and shunt resistance of the microphone and its cable.

51. Let $\delta_1(t)$ be the electric response of the microphone, due to a unit impressed pressure wave, and assume that $\delta_1(t)$ is appreciable only over the interval $t = 0$ to $t = \epsilon_1$. Then, for an arbitrary impressed pressure wave $p(t)$ the derivative $p'(t)$ of which does not vary much over an interval ϵ_1, the response of the microphone is approximately proportional to $p'(t)$.

52. To show this and obtain the degree of approximation, it follows from DuHamel's theorem that, where $e(t)$ is the response to an arbitrary impressed wave $p(t)$,

$$e(t) = p(0)\,\delta_1(t) + \int_0^t \delta_1(t-\lambda)\, p'(\lambda)\, d\lambda \qquad (1)$$

Now the only contribution to this integral which is appreciable is over an interval ϵ_1, and since $p'(t)$ does not change much in such an interval, it can be well represented by a Taylor series in powers of $(\lambda - t)$. Hence, assuming $p(0) = 0$, as it will be for any physical wave

$$e(t) = \int_0^\tau \delta_1(t-\lambda)\left[\, p'(t) + (\lambda - t)\, p''(t) + \frac{(\lambda-t)^2}{2}\, p'''(t) + \frac{(\lambda-t)^3}{6}\, p^{IV}(t) + \cdots \right] d\lambda \qquad (2)$$

Let $t - \lambda = x$, $dx = -d\lambda$

$$e(t) = -p'(t)\int_t^0 \delta_1(x)\,dx + p''(t)\int_t^0 x\,\delta_1(x)\,dx - \frac{p'''(t)}{2}\int_t^0 x^2\,\delta_1(x)\,dx + \frac{p^{IV}(x)}{6}\int_t^0 x^3\,\delta_1(x)\,dx - \cdots \qquad (3)$$

[redacted]

For $t > t_1$, the integrals are essentially the moments of $\delta_1(t)$. Hence expressing

$$\int_0^\infty t^n \delta_1(t)\,dt \quad \text{by} \quad S\,\bar{\tau}^n$$

where

$$S = \int_0^\infty \delta_1(t)\,dt$$

$$e(t) = S\left(p'(t) - \bar{\tau}\,p''(t) + \frac{\bar{\tau}^2}{2}p'''(t) - \frac{\bar{\tau}^3}{6}p^{IV}(t) + \cdots\right) \qquad (4)$$

Taking advantage of the fact that

$$p'(t-\bar{\tau}) = p'(t) - \bar{\tau}\,p''(t) + \frac{\bar{\tau}^2}{2}p'''(t) - \frac{\bar{\tau}^3}{6}p^{IV}(t) + \cdots \qquad (5)$$

The first two terms of $e(t)$ can be combined to express $e(t)$ in terms of a time delay and corrections depending on $\bar{\tau}^2 - \bar{\tau}^3$.

$$e(t) = S\left(p'(t-\bar{\tau}) + \frac{\bar{\tau}^2 - \bar{\tau}^2}{2}p'''(t) - \frac{\bar{\tau}^3 - \bar{\tau}^3}{6}p^{IV}(t) + \cdots\right) \qquad (6)$$

Since $e(t)$ is the observed function, it is more useful to have the unknown function $p'(t-\bar{\tau})$ expressed as proportional to $e(t)$ plus corrections depending on $e(t)$.

Taking the derivative twice of the expression for $e(t)$ given in (4), one gets $e''(t) \simeq S\,p'''(t)$. This is substituted in (6), and solving for $p'(t-\bar{\tau})$ one gets

$$p'(t-\bar{\tau}) = \frac{1}{S}\left(e(t) - \frac{\bar{\tau}^2 - \bar{\tau}^2}{2}e''(t)\right) \qquad (7)$$

dropping terms of the third and higher order. This expression means that the derivative of the pressure wave $p'(t) = \partial p/\partial r$ is proportional to the response $e(t)$ of the microphone, or oscillogram trace, with a delay of $\bar{\tau}$. The percent error may be estimated from the ratio of the second term on the right to the first. For a sinusoid, the interpretation that the response is proportional to the derivative of the impressed wave fails when

$$4\pi^2\nu^2\,\frac{\bar{\tau}^2 - \bar{\tau}^2}{2} \simeq 1$$

(See Para. 54)

53. Consider the case when the imperfect response of the amplifier is taken into account. Let the response of the amplifier to a step voltage be $1(t) - \delta_2(t)$ where $1(t)$ is Heaviside's step function and $\delta_2(t) \simeq 1$ at $t=0$, is appreciable over a range up to

$t = \epsilon_2$, and is not otherwise restricted. Then the combined response of the microphone-amplifier system to a unit pressure wave is $\delta_3(t)$, where

$$\delta_3(t) = \delta_1(0)\left[1(t) - \delta_2(t)\right] + \int_0^\tau \left[\;\right](t-\lambda) - \delta_2(t-\lambda)\Big]\delta_1'(\lambda)\,d\lambda$$

The input impedance of the amplifier is assumed to be taken into account in $\delta_1(t)$. It is intended to show that $\delta_3(t)$ is a function which becomes inappreciable after a time $\epsilon_3 = \epsilon_1 + \epsilon_2$. Hence, by the analysis of the previous paragraph, the microphone-amplifier system also responds to the derivative of an arbitrary impressed pressure wave, provided it does not change appreciably over a time $\epsilon_3 = \epsilon_1 + \epsilon_2$.

$$\delta_3(t) = \delta_1(0) - \delta_1(0)\,\delta_2(t) + \delta_1(\lambda)\Big|_0^\tau - \int_0^\tau (t-\lambda)\,\delta_1'(\lambda)\,d\lambda$$

$$= \delta_1(0) - \delta_1(0)\,\delta_2(t) + \delta_1(\tau) - \delta_1(0) - \delta_2(t-\lambda)\,\delta_1(\lambda)\Big|_{\lambda=0}^{\lambda=\tau}$$

$$- \int_0^t \delta_1(\lambda)\,\delta_2'(t-\lambda)\,d\lambda$$

$$\therefore \quad \delta_3(t) = -\int_0^\tau \delta_1(\lambda)\,\delta_2'(t-\lambda)\,d\lambda$$

Consider this function of t to be appreciable in those regions where either factor in the integrand is appreciable. If neither is appreciable, the contribution to the integral is considered negligible and the function as a function of t is considered negligible. Consider the first factor; it is appreciable up to a point where its argument is ϵ_1. At that point, in the second factor $t - \lambda = \tau - \epsilon_1$. Considered as a function of t, this is significant where $t = \epsilon_1 = \epsilon_2$, or $t = \epsilon_1 + \epsilon_2$, i.e. as a function of t the integral is negligible beyond $t = \epsilon_1 + \epsilon_2$. A similar conclusion is reached by considering the second factor. The second is appreciable up to $t - \lambda = \epsilon_2$, or to $\lambda = \tau - \epsilon_2$ in the first factor. The first factor becomes inappreciable when its argument $\lambda = \tau - \epsilon_2 = \epsilon_1$ or $t = \epsilon_1 + \epsilon_2$, considered as a function of t. Hence, the entire function is negligible past $t = \epsilon_1 + \epsilon_2$. Therefore, the response of the microphone-amplifier system is also proportional to the time derivative of the impressed wave.

54. These considerations can be used to estimate the error committed in interpreting the oscillograms as proportional to $\partial p / \partial t$, using the observed calibration curve of the microphone. Here the impressed wave is a sinusoid, and the observed calibration is for rms values of pressure, and voltage. Since

$$p'(t - \bar{\tau}) = \frac{1}{S}\left(e(t) - \frac{\bar{\tau}^2 - \bar{\tau}^2}{2}\,e''(t)\right)$$

if $\quad e(t) = A(\nu)\sin 2\pi\nu t \qquad e''(t) = -A(\nu)\,4\pi^2\nu^2 \sin 2\pi\nu t$

$$p(t) = B\sin(2\pi\nu t - \varphi) \qquad p'(t) = 2\pi\nu\, B\cos(2\pi\nu t - \varphi)$$

[redacted]

[redacted]

then for rms values

$$\frac{S|p'|}{|e|} = \frac{S|p|2\pi\nu}{|e|} = \frac{2\pi\nu SB}{A(\nu)} = 1 + \frac{4\pi^2\nu^2(\bar{\tau}^2 - \bar{\tau}_i^2)}{2}$$

The value of the right hand side gives the deviation, if expressed in db, of the observed calibration curve from a straight line (Plate 2). If one takes the deviation at 5000 cycles as 2.5 db, then the above expression gives

$$\frac{\bar{\tau}^2 - \bar{\tau}_i^2}{2} = 3.35 \times 10^{-10} \text{ sec}^2$$

For purposes of estimating the error for the oscillograms, assume the first peaks to be sinusoidal, with a time of rise from 1/2 to full max = 1/4 (1/ν), which is a fair approximation. 5

For example, if the time of rise is 100 μsecs, (air bubble~10 cu mm) See plates 4, 5, 6, 7.

$$\frac{4\pi\nu^2(\bar{\tau}^2 - \bar{\tau}_i^2)}{2} = \frac{4\pi^2}{(400)^2} \cdot 10^{12} \cdot 3.35 \cdot 10^{-10} = 8.3\%$$

If the time of rise were 50 μsecs the error would be $\simeq$33% (air bubbles $\simeq$1 cu mm). These figures indicate the limits on the interpretation of the oscillogram trace as proportional to $\partial p/\partial r$. The error as calculated from assuming the amplifier response to be $1-\exp(-t/\tau_A)$, the microphone response to be $\exp(-t/\tau_M)$ is considerably less than the above. This indicates that the time required for the pressure wave to traverse the microphone is not negligible, or that mechanical coupling to the crystal prolongs its effective time constant. T_A as measured by a square wave generator was 6.7 μ secs. $RC = T_M = 5.9\mu$ secs.

55. To convert the deflections on the oscillograms in millivolts to dynes / cm^{2}sec, one should use a constant determined from the calibration curve rather than one computed from the piezo-electric constant of the crystal and its RC. For the straight part of the calibration curve, by paragraph 54, $S|p|2\pi\nu = |e|$.
For ν = 1000, p = 1 dyne/cm^2, one can find S=2.13 x 10^{-12} volts/dyne/cm^2 sec corresponding to $|e|$ equals 157.5 db below 1 volt/dyne cm^2. Since $|p'| = |e|S$, a one millivolt deflection on the oscillogram, amplifier gain zero, corresponds to 0.47 x 10^9 dynes/cm^2 sec, or 0.47x10^{-3} atmospheres per microsec.

56. The maximum "hydrostatic" pressure sustained by the vessel as a whole would depend on the integral of the oscillogram trace, carried out to the point B of the sketch (para. 30). For example in Plate 17, No.1, a deflection of 5 millivolts for 1000μ secs means a maximum pressure of 2.3 atmospheres, approximately. This is of the order of magnitude of results obtained by Baker (1) using an electric stress recorder. This maximum pressure is approximately that plotted for the slowest mode of vibration in Plates 14 and 15, since the integral of the oscillogram depends primarily on the magnitude of the slowest mode.

APPENDIX II - Discussion of the Incompressible Theory

57. The equation of motion (2) for a spherical cavity in an infinite medium is

$$2\pi\rho\, a^3\left(\frac{da}{dt}\right)^2 + \frac{4\pi}{3}a^3 P_\infty + G(a) = E \qquad (1)$$

where a = instantaneous radius of cavity

P_∞ = hydrostatic pressure

$G(a)$ = gas energy = $\frac{4\pi P_\infty}{3(\gamma-1)}\left(\frac{a_1}{a}\right)^{3\gamma} a^3$

E = total energy = $\frac{4\pi}{3} R_o^3 P_\infty$

R_o = maximum radius of cavity

a_1 = radius of the cavity at which the gas pressure equals the hydrostatic pressure. This is not the measured radius of the air bubble in these experiments, since the expansion of the cavity took place isothermally, the collapse adiabatically. The volume was measured, and the volume V_1 referring to the radius a_1 are related by the formula,

$$\left(\frac{V_1}{\frac{4}{3}\pi R_o^3}\right)^\gamma = \frac{V}{\frac{4}{3}\pi R_o^3} = \frac{V}{E_{cu\ mm}}$$

58. The above equation can be rewritten in the dimensionless variables

$$y = \frac{a}{R_o}, \quad x = \frac{t}{R_o}\sqrt{\frac{P_\infty}{\rho}}, \quad \text{and} \quad \frac{V_1}{\frac{4}{3}\pi R_o^3} = \alpha$$

Then

$$y^3\left(\frac{dy}{dx}\right)^2 + \frac{2}{3}y^3 + \frac{2\alpha^\gamma}{3(\gamma-1)}\cdot\frac{1}{y^{3\gamma}} = \frac{2}{3} \qquad (2)$$

59. As is mentioned in paragraph 43, it is desired to determine the value of V/E cu mm for which $da/dt = c$, the velocity of sound, at the same instant that the gas pressure equals the hydrostatic pressure. This is done by placing $y = \alpha^{1/3}$ (then $a = a_1$), $dy/dx = c\sqrt{\rho/P_\infty}$ (since then $da/dt = c$) in equation (2) above, and solving for the value of α. This gives, almost independently of γ

$$\alpha \simeq \frac{2}{3}\frac{P_\infty}{\rho c^2} = 0.33 \times 10^{-4}$$

whence, for $\gamma = 1.40$ (air)

$$\frac{V}{E_{cu\ mm}} = \alpha^\gamma = 5.5 \times 10^{-7}$$

verifying the value quoted in paragraph 44.

60. Equation (2) can also be used to solve for the value of V/E cu mm for which the maximum velocity of collapse is

the velocity of sound, as mentioned in paragraph 45. The maximum value of dy/dx (or da/dt) is given from

$$\left(\frac{dy}{dv}\right)^2 = \frac{2}{3y^3} - \frac{2}{3} - \frac{2}{3(\gamma-1)} \cdot \frac{\alpha^\gamma}{y^{3\gamma}} \qquad (3)$$

$$\frac{d}{dy}\left(\frac{dy}{dx}\right)^2 = -\frac{2}{y^4} + \frac{2}{3} \cdot \frac{\alpha^\gamma}{(\gamma-1)} \cdot \frac{3\gamma}{y^{3\gamma+1}} = 0 \qquad (4)$$

from which

$$y_{\left(\frac{dy}{dx}\right)_{max}} = \alpha^{\frac{\gamma}{3(\gamma-1)}} \left(\frac{\gamma}{\gamma-1}\right)^{\frac{1}{3(\gamma-1)}} \qquad (5)$$

(5) substituted in (3) gives

$$\left(\frac{dy}{dx}\right)^2_{max} = \frac{2(\gamma-1)^{\frac{1}{\gamma-1}}}{3\,\alpha^{\frac{\gamma}{\gamma-1}}} \left[\left(\frac{1}{\gamma}\right)^{\frac{1}{\gamma-1}} - \left(\frac{1}{\gamma}\right)^{\frac{\gamma}{\gamma-1}}\right] = \frac{\rho c^2}{P_\infty}$$

From this one can solve α, and get, for $\gamma = 1.40$ the desired value of V/E cu mm $= \alpha^\gamma = 2.8 \times 10^{-3}$, verifying the result quoted in paragraph 50.

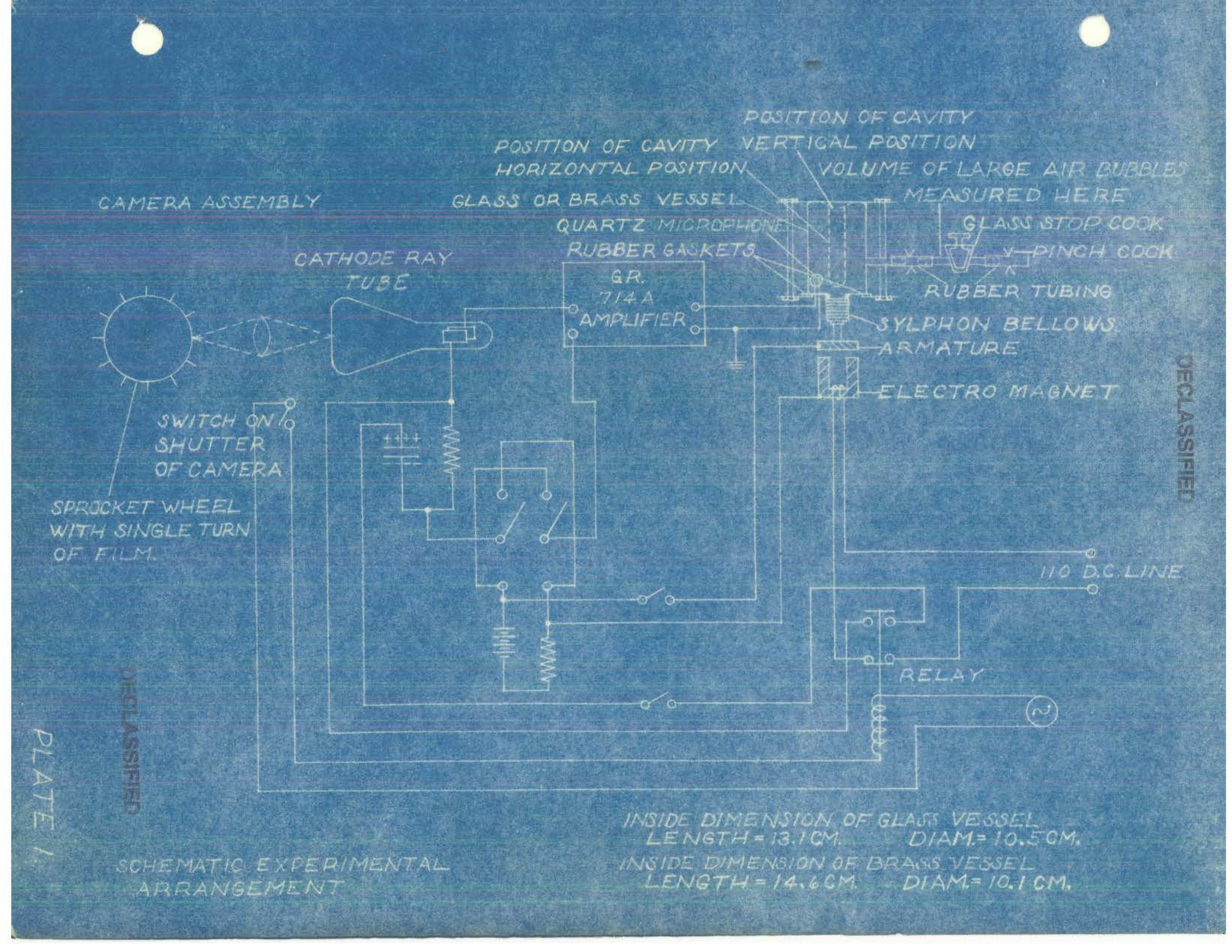
POSITION OF CAVITY
VERTICAL POSITION
POSITION OF CAVITY
HORIZONTAL POSITION
VOLUME OF LARGE AIR BUBBLES
MEASURED HERE
CAMERA ASSEMBLY
GLASS OR BRASS VESSEL
QUARTZ MICROPHONE
GLASS STOP COCK
RUBBER GASKETS
PINCH COCK
CATHODE RAY
TUBE
G.R.
714 A
AMPLIFIER
RUBBER TUBING
SYLPHON BELLOWS
ARMATURE
ELECTRO MAGNET
SWITCH ON
SHUTTER
OF CAMERA
SPROCKET WHEEL
WITH SINGLE TURN
OF FILM.
110 D.C. LINE
RELAY
DECLASSIFIED
DECLASSIFIED
PLATE I
SCHEMATIC EXPERIMENTAL
ARRANGEMENT
INSIDE DIMENSION OF GLASS VESSEL
LENGTH = 13.1 CM. DIAM. = 10.5 CM.
INSIDE DIMENSION OF BRASS VESSEL
LENGTH = 14.6 CM. DIAM. = 10.1 CM.

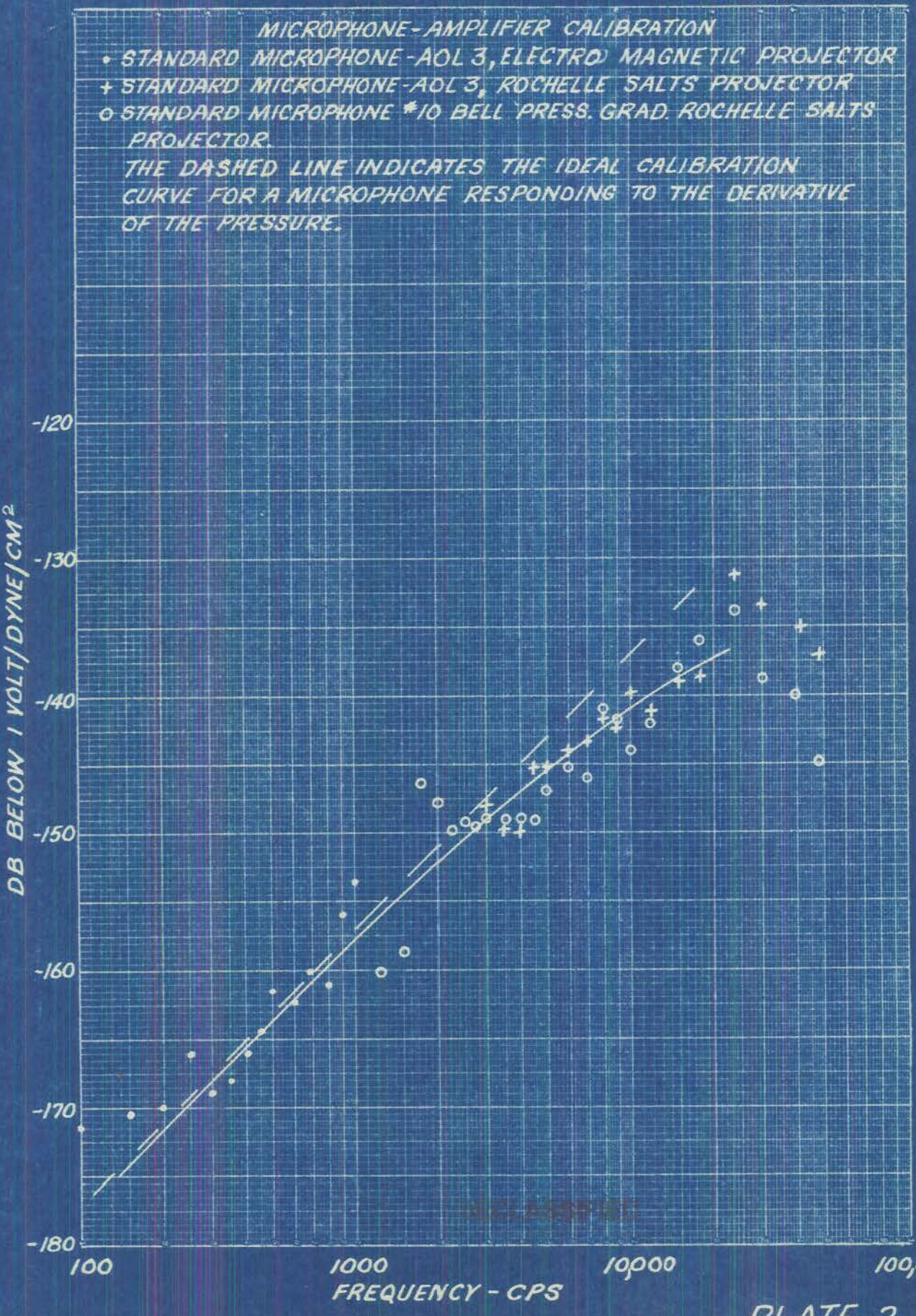

PLATE 2

U. S. NAVAL RESEARCH LABORATORY
BELLEVUE, D. C.

DATE

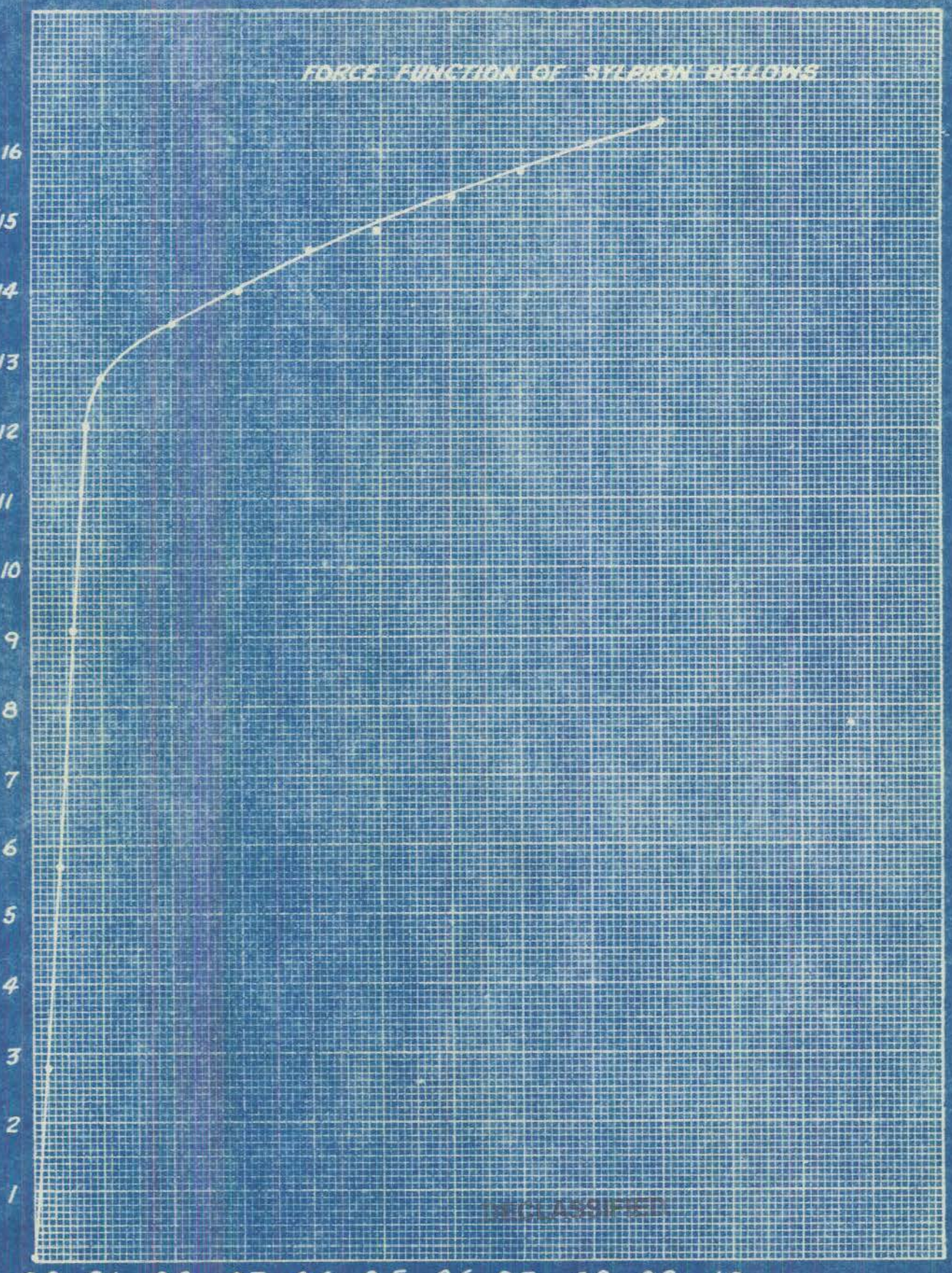

PLATE 3

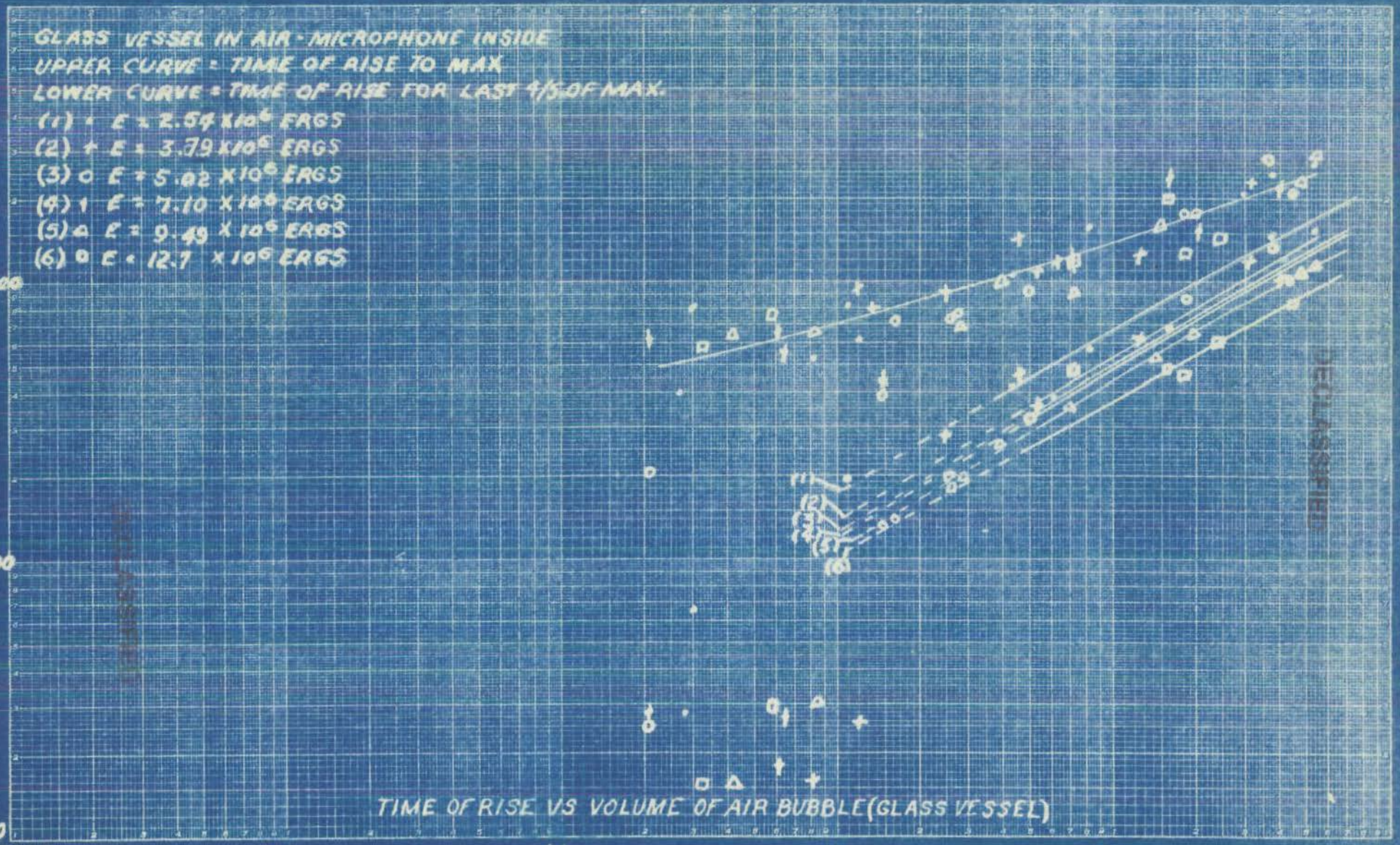
GLASS VESSEL IN AIR - MICROPHONE INSIDE
UPPER CURVE = TIME OF AISE TO MAX
LOWER CURVE = TIME OF RISE FOR LAST 4/5 OF MAX.
(1) • E = 2.54 X10^6 ERGS
(2) + E = 3.79 X10^6 ERGS
(3) ○ E = 5.02 X10^6 ERGS
(4) ▪ E = 7.10 X10^6 ERGS
(5) △ E = 9.49 X10^6 ERGS
(6) □ E = 12.7 X10^6 ERGS
1000
100
10
TIME IN MICRO SECS.
0.01
0.1
1.0
10
100
1000
V = VOLUME OF AIR BUBBLE CU.MM
TIME OF RISE VS VOLUME OF AIR BUBBLE (GLASS VESSEL)

PLATE 4

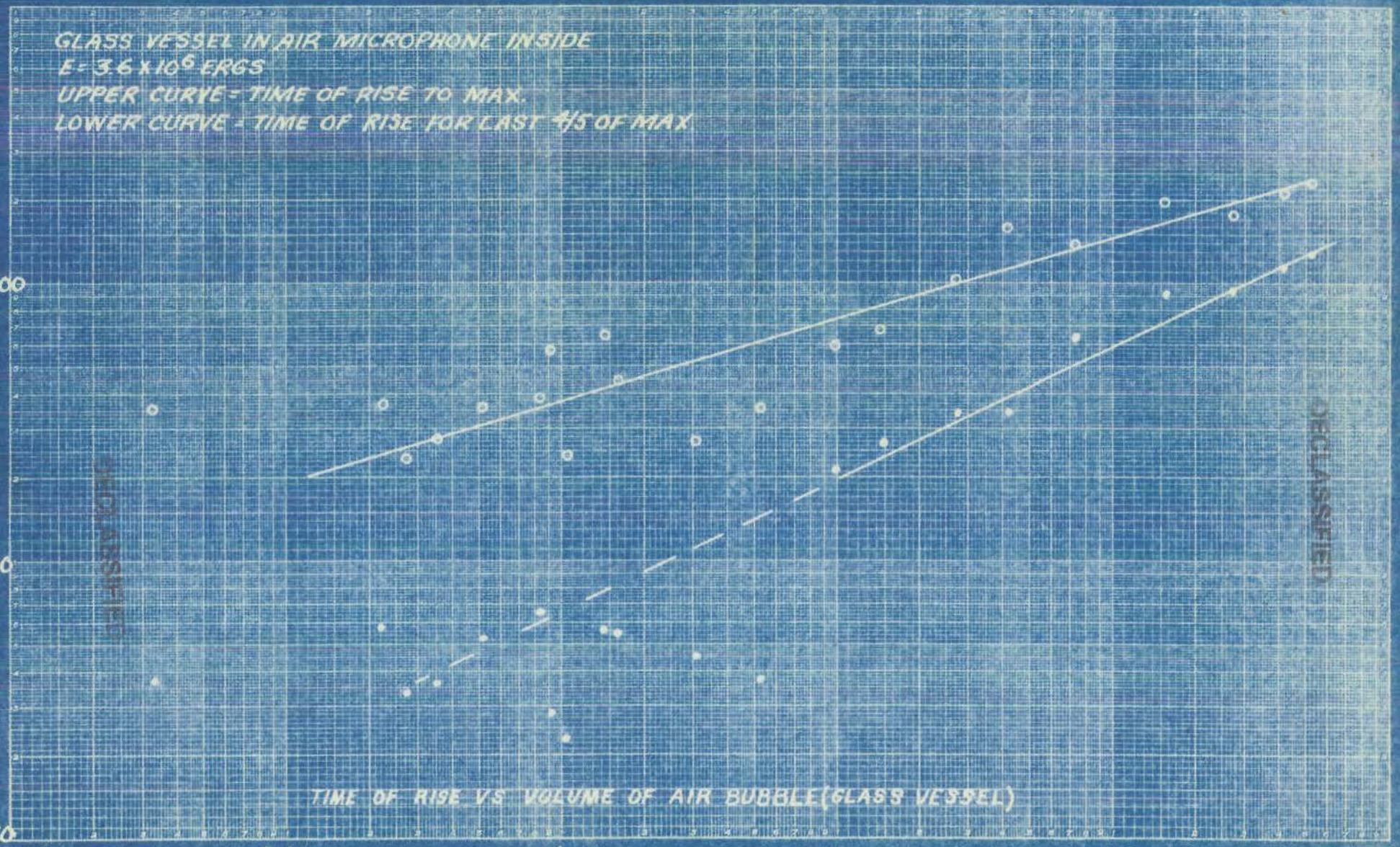
GLASS VESSEL IN AIR MICROPHONE INSIDE
E = 3.6 x 10⁶ ERGS
UPPER CURVE = TIME OF RISE TO MAX.
LOWER CURVE = TIME OF RISE FOR LAST 4/5 OF MAX
1000
100
10
TIME IN MICRO SECS.
0.01
0.1
1
10
100
1000
V = VOLUME OF AIR BUBBLE CU. MM
TIME OF RISE VS VOLUME OF AIR BUBBLE (GLASS VESSEL)
DECLASSIFIED
DECLASSIFIED

PLATE 5

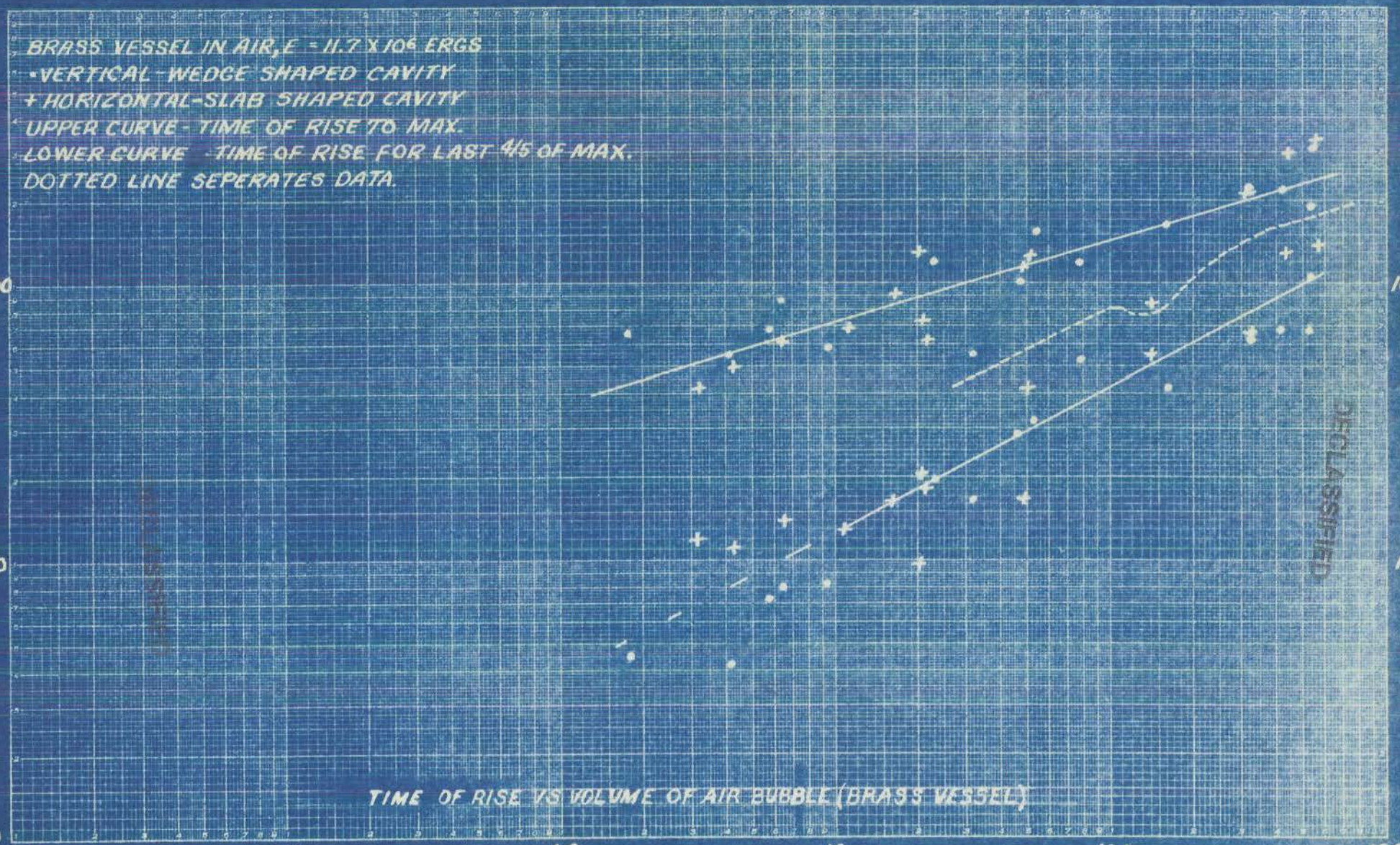
BRASS VESSEL IN AIR, E = 11.7 X 10⁶ ERGS
• VERTICAL - WEDGE SHAPED CAVITY
+ HORIZONTAL-SLAB SHAPED CAVITY
UPPER CURVE - TIME OF RISE TO MAX.
LOWER CURVE - TIME OF RISE FOR LAST 4/5 OF MAX.
DOTTED LINE SEPERATES DATA.
1000
100
10
TIME IN MICRO SECS.
0.01
0.1
1.0
10
100
1000
V = VOLUME OF AIR BUBBLE CU. MM.
TIME OF RISE VS VOLUME OF AIR BUBBLE (BRASS VESSEL)

PLATE 9

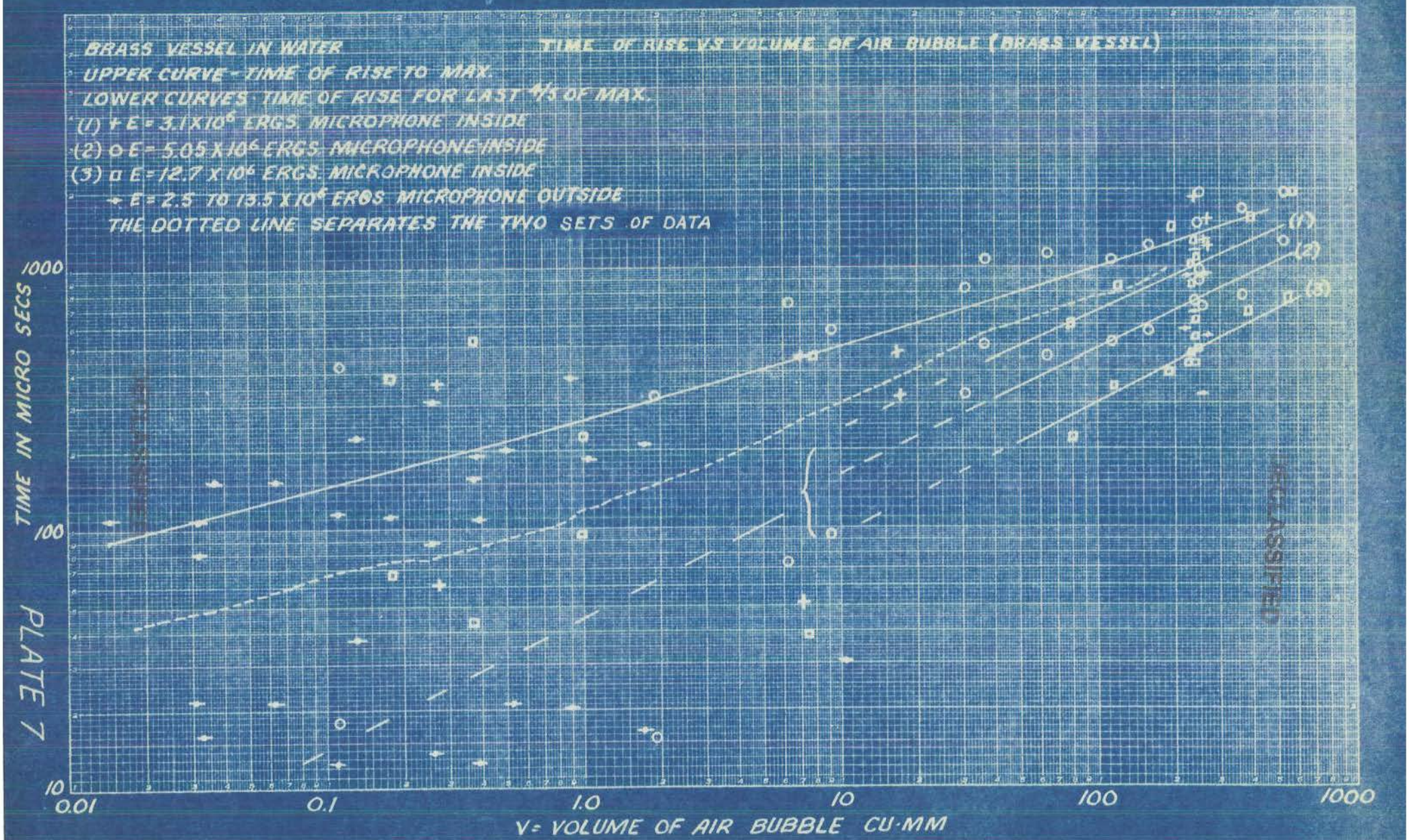
BRASS VESSEL IN WATER
UPPER CURVE - TIME OF RISE TO MAX.
LOWER CURVES TIME OF RISE FOR LAST 4/5 OF MAX.
(1) + E = 3.1 X 10⁶ ERGS. MICROPHONE INSIDE
(2) ○ E = 5.05 X 10⁶ ERGS. MICROPHONE INSIDE
(3) □ E = 12.7 X 10⁶ ERGS. MICROPHONE INSIDE
→ E = 2.5 TO 13.5 X 10⁶ ERGS MICROPHONE OUTSIDE
THE DOTTED LINE SEPARATES THE TWO SETS OF DATA
TIME OF RISE VS VOLUME OF AIR BUBBLE (BRASS VESSEL)
TIME IN MICRO SECS
1000
100
10
0.01
0.1
1.0
10
100
1000
V = VOLUME OF AIR BUBBLE CU·MM
(1)
(2)
(3)
CONFIDENTIAL
UNCLASSIFIED

PLATE 7

PLATE 8

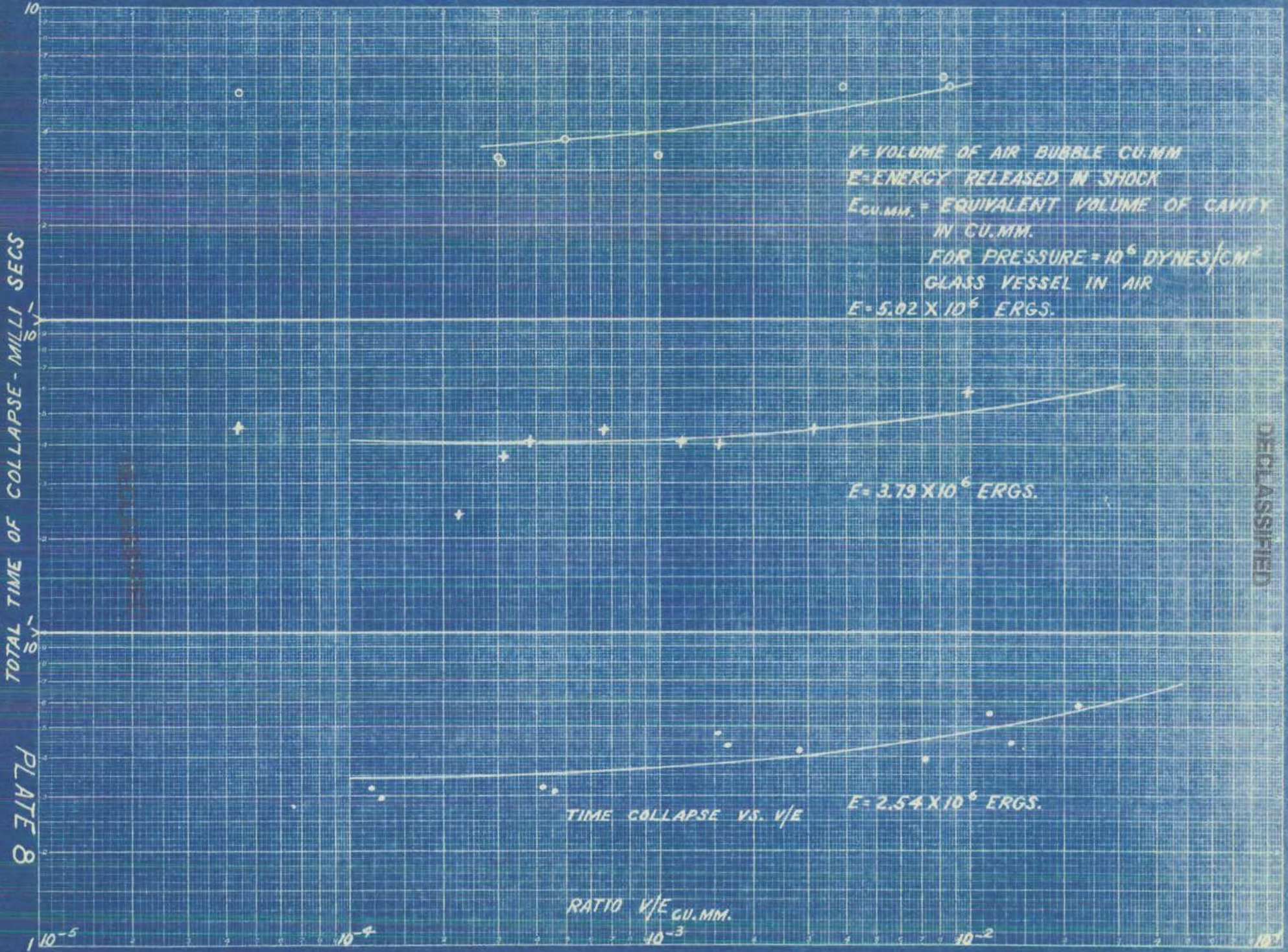

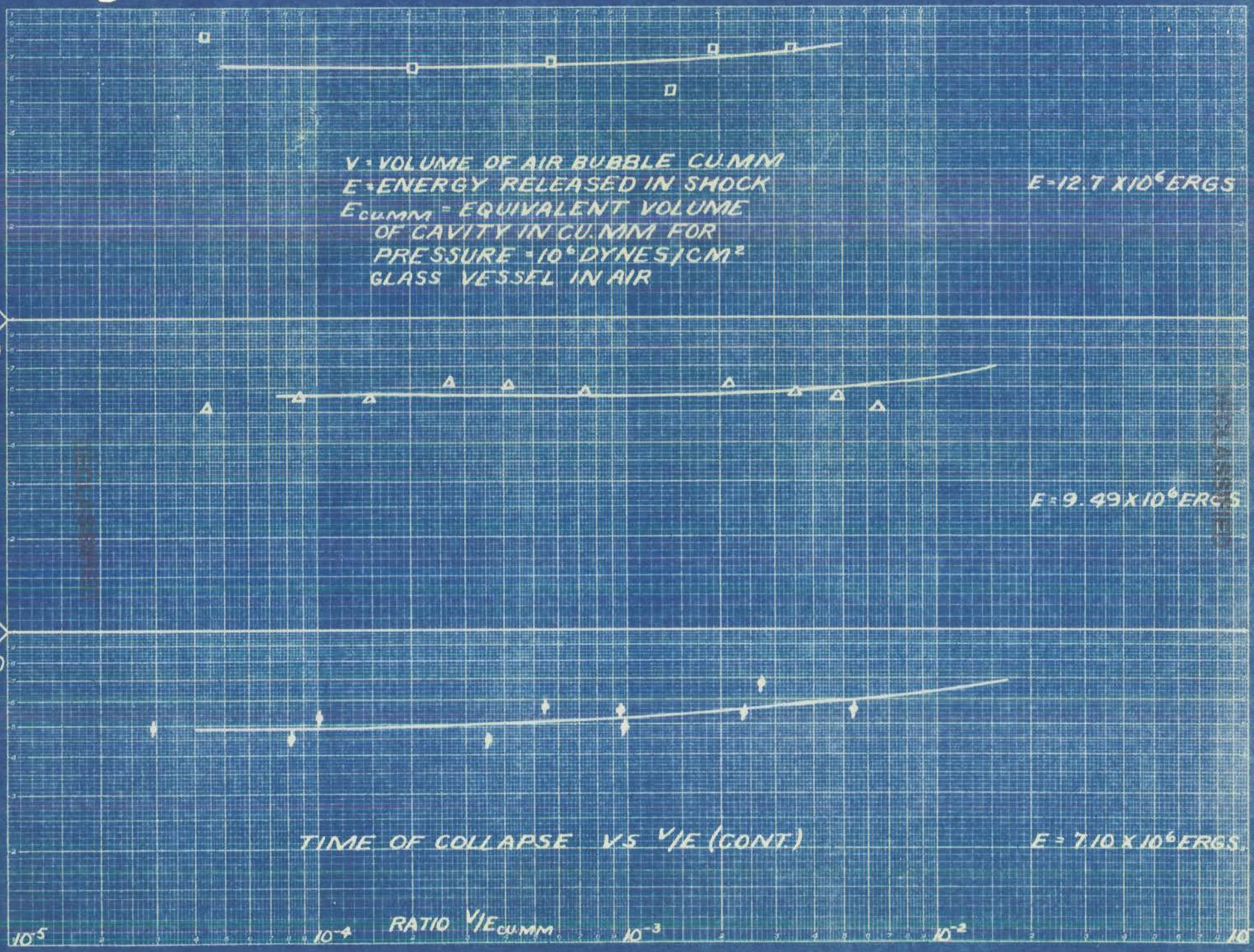
V = VOLUME OF AIR BUBBLE CU.MM
E = ENERGY RELEASED IN SHOCK
E cu.mm = EQUIVALENT VOLUME OF CAVITY IN CU.MM FOR PRESSURE = 10⁶ DYNES/CM²
GLASS VESSEL IN AIR
E = 12.7 X 10⁶ ERGS
E = 9.49 X 10⁶ ERGS
E = 7.10 X 10⁶ ERGS.
TIME OF COLLAPSE V.S V/E (CONT)
TOTAL TIME OF COLLAPSE MILLI-SECS
RATIO V/E cu.mm
10⁻⁵
10⁻⁴
10⁻³
10⁻²
10⁻¹

PLATE 9

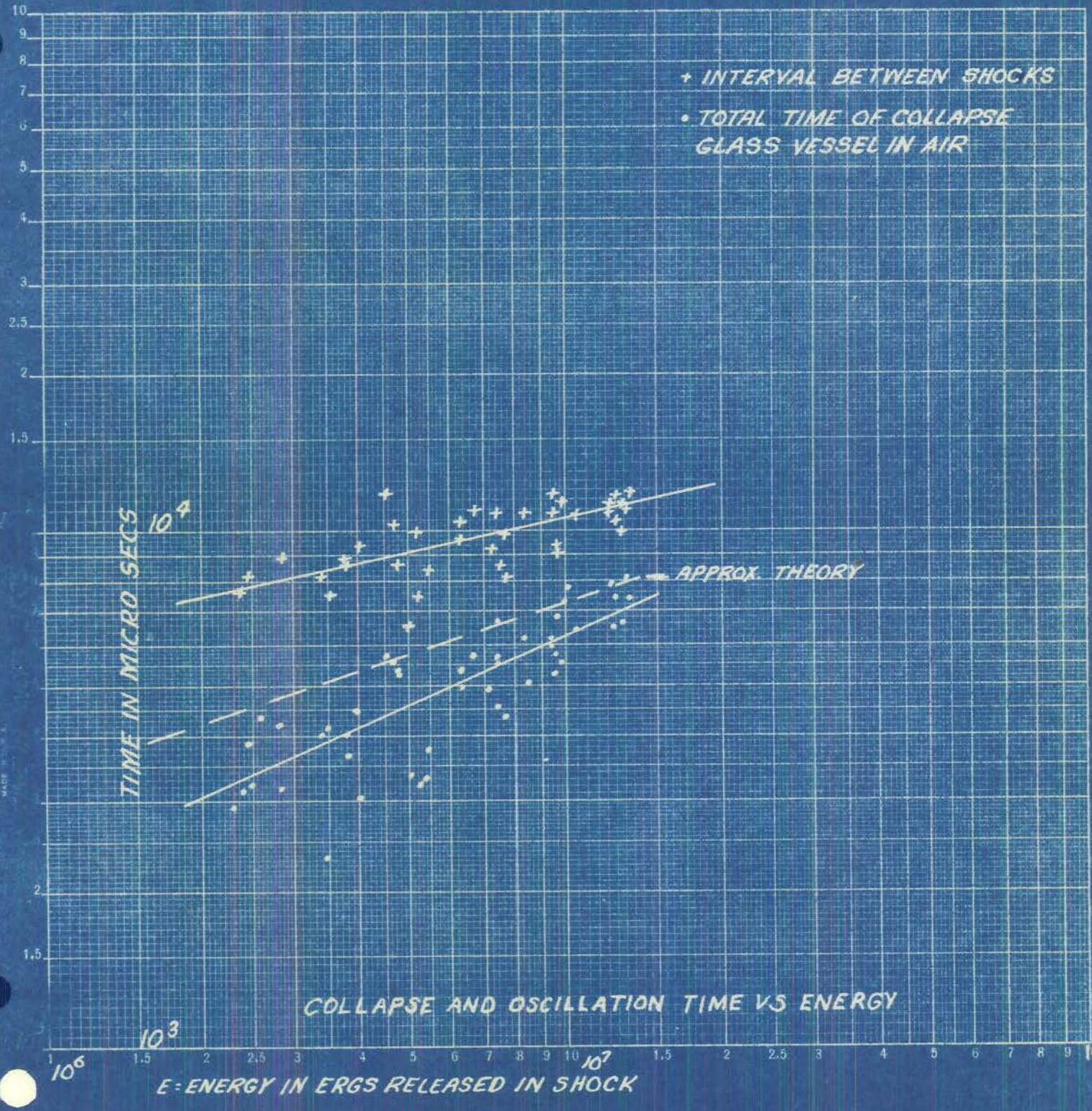

KEUFFEL & ESSER CO., N. Y. NO. 359-110
Logarithmic, 2 × 2 Cycles.

COLLAPSE AND OSCILLATION TIME VS ENERGY

PLATE 10

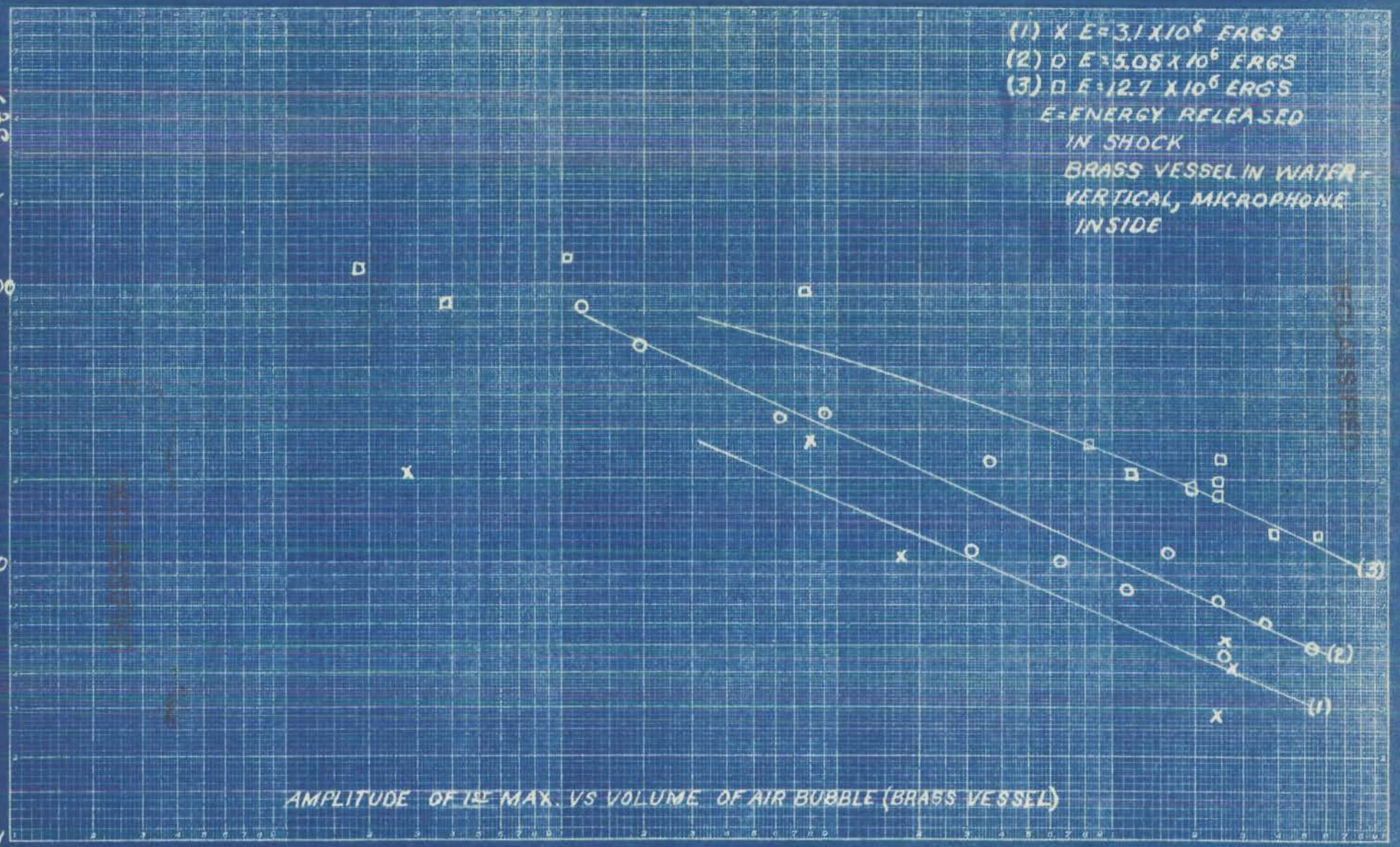

AMPLITUDE OF 1ST MAX. VS VOLUME OF AIR BUBBLE (BRASS VESSEL)

PLATE 11

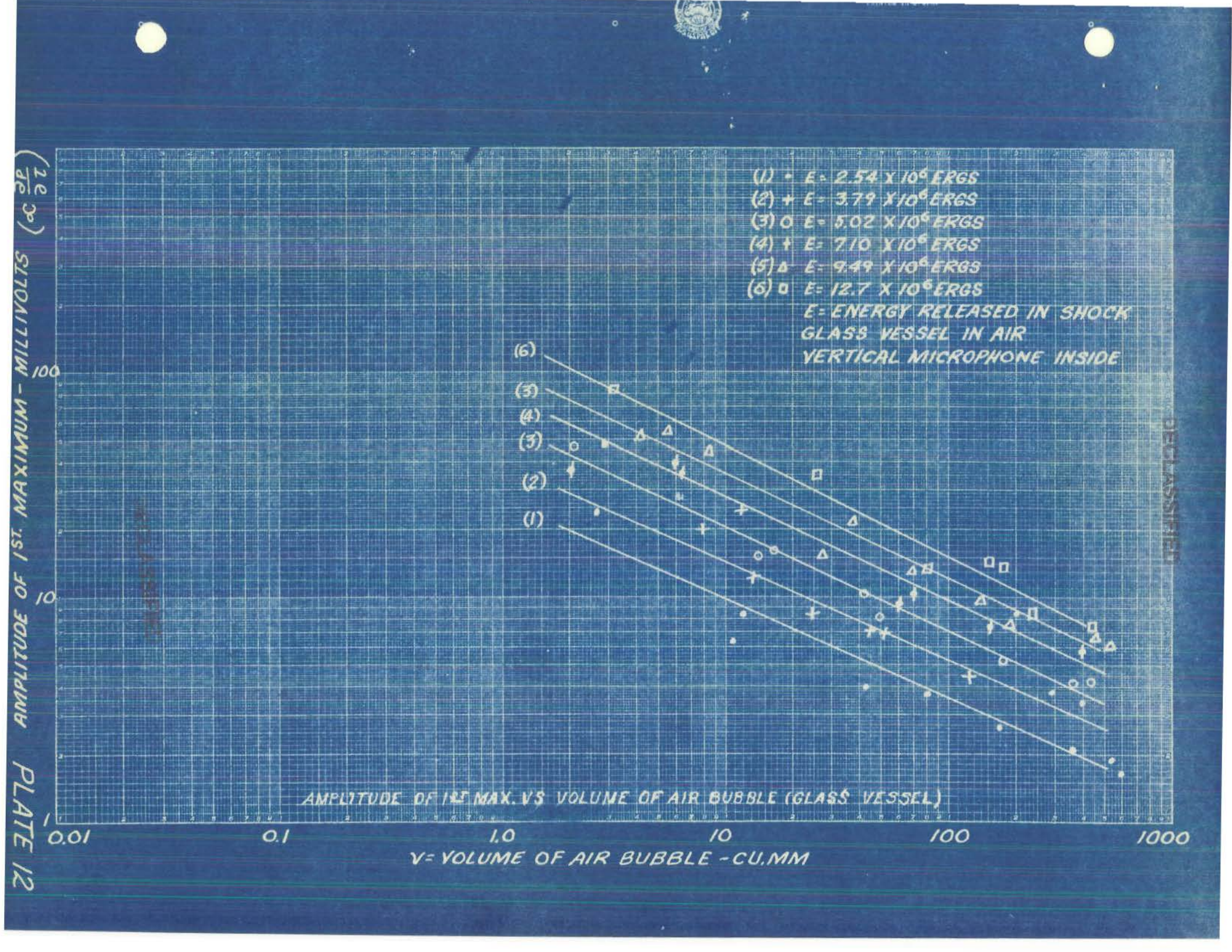
(1) • E= 2.54 X 10⁶ ERGS
(2) + E= 3.79 X 10⁶ ERGS
(3) O E= 5.02 X 10⁶ ERGS
(4) † E= 7.10 X 10⁶ ERGS
(5) Δ E= 9.49 X 10⁶ ERGS
(6) □ E= 12.7 X 10⁶ ERGS
E= ENERGY RELEASED IN SHOCK
GLASS VESSEL IN AIR
VERTICAL MICROPHONE INSIDE
(6)
(5)
(4)
(3)
(2)
(1)
AMPLITUDE OF 1ST MAX. VS VOLUME OF AIR BUBBLE (GLASS VESSEL)
AMPLITUDE OF 1ST. MAXIMUM - MILLIVOLTS (2e/e∞)
100
10
1
0.01
0.1
1.0
10
100
1000
V= VOLUME OF AIR BUBBLE - CU.MM
DECLASSIFIED
PLATE 12

PLATE 13

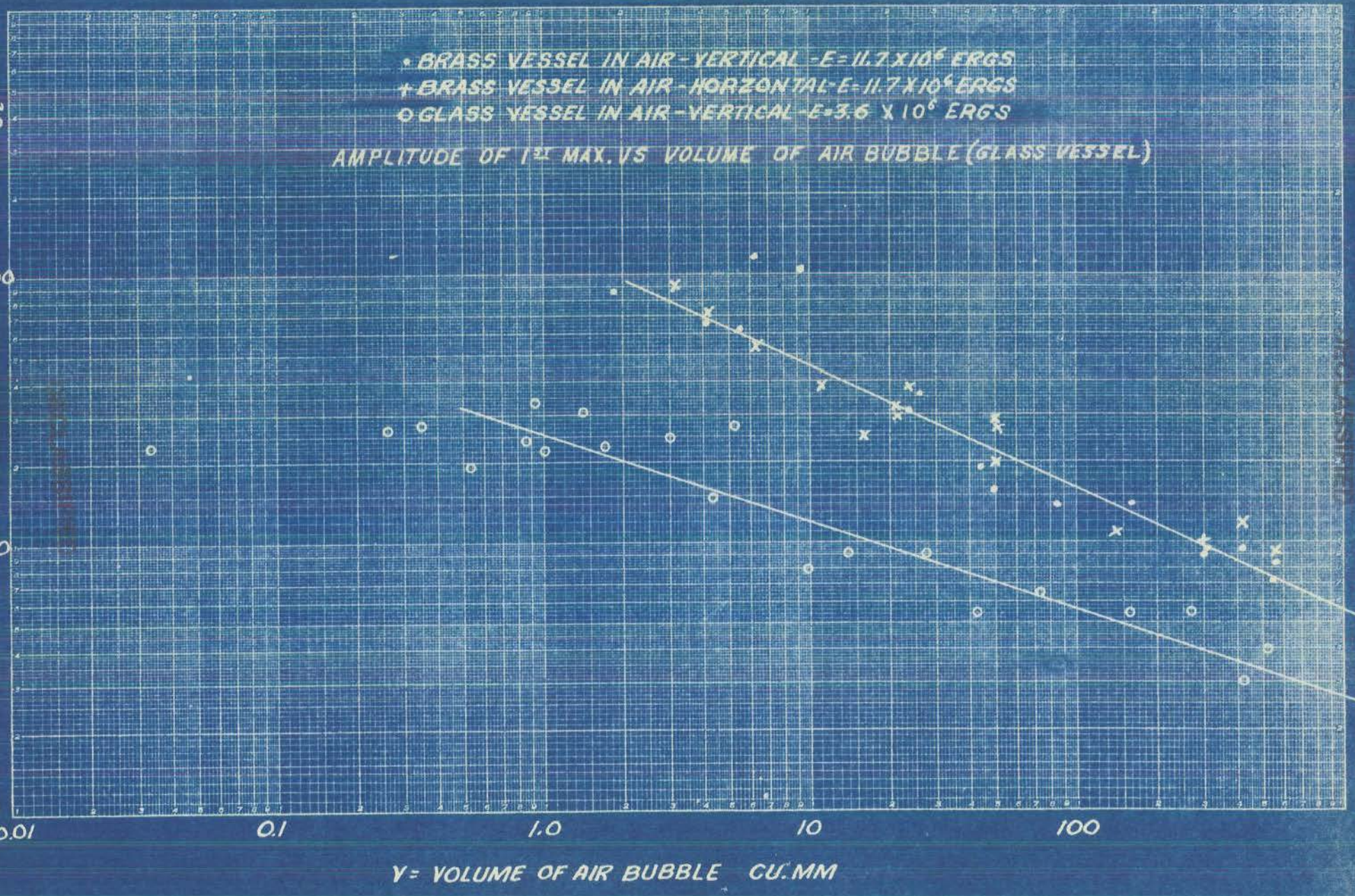
• BRASS VESSEL IN AIR - VERTICAL - E = 11.7 X 10⁶ ERGS
+ BRASS VESSEL IN AIR - HORIZONTAL - E = 11.7 X 10⁶ ERGS
○ GLASS VESSEL IN AIR - VERTICAL - E = 3.6 X 10⁶ ERGS
AMPLITUDE OF 1ST MAX. VS VOLUME OF AIR BUBBLE (GLASS VESSEL)
AMPLITUDE OF 1ST MAXIMUM MILLI VOLTS (dp/dt)
100
10
1
0.01
0.1
1.0
10
100
Y = VOLUME OF AIR BUBBLE CU. MM

PLATE 14

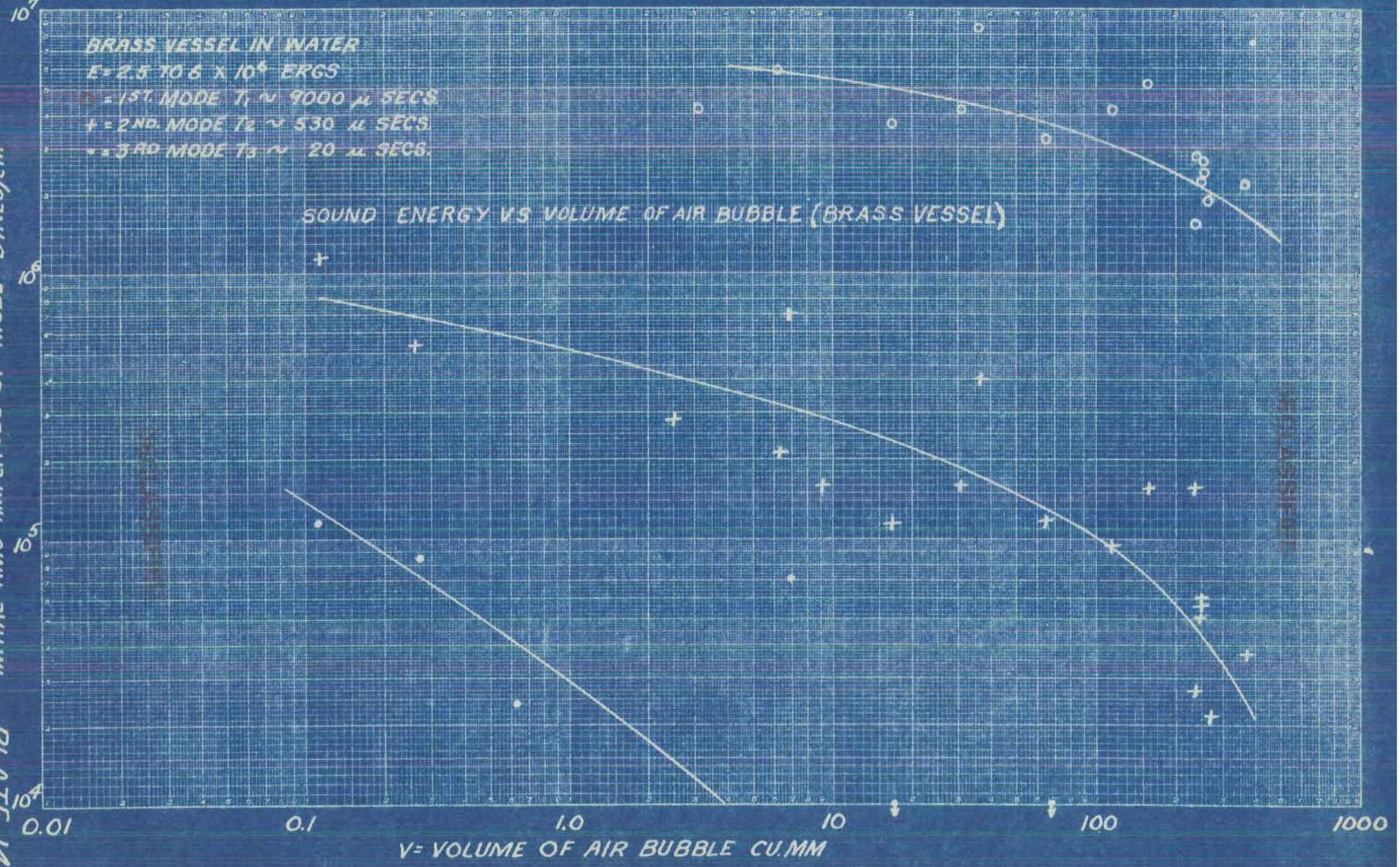
BRASS VESSEL IN WATER
E = 2.5 TO 6 X 10⁴ ERGS
o = 1ST. MODE T1 ~ 9000 μ SECS.
+ = 2ND. MODE T2 ~ 530 μ SECS.
• = 3RD MODE T3 ~ 20 μ SECS.
SOUND ENERGY V.S. VOLUME OF AIR BUBBLE (BRASS VESSEL)
INITIAL RMS AMPLITUDE OF MODE DYNES/CM²
10⁷
10⁶
10⁵
10⁴
0.01
0.1
1.0
10
100
1000
V= VOLUME OF AIR BUBBLE CU.MM

Oscillograms of shocks in glass vessel in air - microphone inside. Vertical position. Low energy group. 0 - release of armature or start of collapse. 1 - first shock, 2 - second shock, etc.

B = volume of air bubble. E = energy released in blow.

1) #52 4-3-42 B = 538 cu mm E = 2.45 x 10^6 ergs. x scale: 123 μsec/mm, y scale: 1.1 mlv/mm

2) #51 4-3-42 B = 298 cu mm E = 2.6 x 10^6 ergs. x scale: 129 μsec/mm, y scale: 1.8 mlv/mm

3) #56 4-3-42 B = 180 cu mm E = 4.65 x 10^6 ergs. x scale: 120 μsec/mm, y scale: 1.9 mlv/mm

4) #50 4-3-42 B = 81 cu mm E = 2.85 x 10^6 ergs. x scale: 116 μsec/mm, y scale: 2.4 mlv/mm

5) #20 4-3-42 B = 46 cu mm E = 3.82 x 10^6 ergs. x scale: 136 μsec/mm, y scale: 2.8 mlv/mm

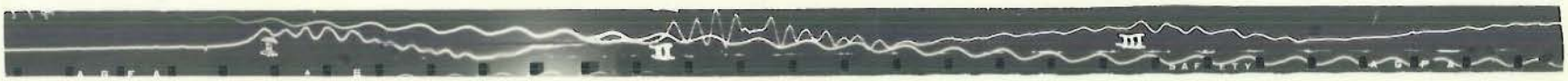

6) #22 3-22-42 B = 41.6 cu mm E = 3.6×10^6 ergs. x scale: 141 μsec/mm, y scale: 2.2 mlv/mm

7) #21 3-22-42 B = 26.9 cu mm E = 3.6×10^6 ergs. x scale: 57 μsec/mm, y scale: 4.7 mlv/mm

8) #46 4-3-42 B = 25 cu mm E = 3.8×10^6 ergs. x scale: 129 μsec/mm, y scale: 5.3 mlv/mm

9) #20 3-22-42 B = 14.6 cu mm E = 3.6×10^6 ergs. x scale: 56 μsec/mm, y scale: 6.3 mlv/mm

10) #15 4-3-42 B = 11 cu mm E = 2.39×10^6 ergs. x scale: 182 μsec/mm, y scale: 3.8 mlv/mm

11) #18 3-22-42 B = 9.8 cu mm E = 3.6×10^6 ergs. x scale: 48 μsec/mm, y scale: 10.5 mlv/mm

PLATE 16B

12) #45 4-3-42 B = 8.0 cu mm E = 3.49×10^6 ergs. x scale: 124 μsec/mm, y scale: 5.7 mlv/mm

13) #15 3-22-42 B = 4.37 cu mm E = 3.6×10^6 ergs. x scale: 58 μsec/mm, y scale: 17 mlv/mm

14) #17 3-22-42 B = 3.06 cu mm E = 3.6×10^6 ergs. x scale: 45 μsec/mm, y scale: 3 mlv/mm

15) #1 4-3-42 B = 2.1 cu mm E = 4.79×10^6 ergs. x scale: 159 μsec/mm, y scale: 31 mlv/mm

16) #11 3-22-42 B = 1.43 cu mm E = 3.6×10^6 ergs. x scale: 61 μsec/mm, y scale: 11mlv/mm

17) #14 3-22-42 B = 0.91 cu mm E = 3.6×10^6 ergs. x scale: 72 μsec/mm, y scale: 10 mlv/mm

PLATE 16C

18) #13 3-22-42 B = 0.52 cu mm E = 3.6×10^6 ergs. x scale: 54 μsec/mm, y scale: 16.7 mlv/mm

19) #9 3-22-42 B = 0.22 cu mm E = 3.6×10^6 ergs. x scale: 59 μsec/mm, y scale: 34 mlv/mm

20) #2 3-22-42 B = 0.034 cu mm E = 2.5×10^6 ergs. x scale: 65 μsec/mm, y scale: 18 mlv/mm

PLATE 16D

Oscillograms of shocks in glass vessel in air. Microphone inside. Vertical position.
High Energy group. 0 - release of armature, or start of collapse. 1 - first shock,
2 - second shock, etc.
B = volume of air bubble. E = energy released in blow.

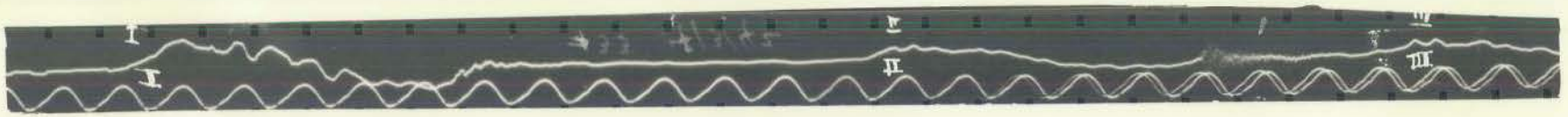

1) #33 4-3-42 B = 441 cu mm E = 13.2 x 10^6 ergs. x scale: 113 μsecs/mm, y scale: 1.7 mlv/mm

2) #65 4-3-42 B = 240 cu mm E = 12.5 x 10^6 ergs. x scale: 127 μsec/mm, y scale: 1.7 mlv/mm

3) #32 4-3-42 B = 155 cu mm E = 12.3 x 10^6 ergs. x scale: 110 μsec/mm, y scale: 3.5 mlv/mm

4) #66 4-3-42 B = 71 cu mm E = 12.1 x 10^6 ergs. x scale: 126 μsec/mm, y scale: 2.6 mlv/mm

5) #24 4-3-42 B = 39 cu mm E = 9.3 x 10^6 ergs. x scale: 173 μsec/mm, y scale: 9.4 mlv/mm

PLATE 17A

6) #31 4-3-42 B = 26 cu mm E = 12.5 x 10^6 ergs. x scale: 118 μsec/mm, y scale: 28 mlv/mm

7) #23 4-3-42 B = 8.5 cu mm E = 9.65 x 10^6 ergs. x scale: 165 μsec/mm, y scale: 28 mlv/mm

8) #36 4-3-42 B = 4.2 cu mm E = 9.5 x 10^6 ergs. x scale; 141 μsec/mm, y scale: 16 mlv/mm

PLATE 17B

Oscillograms of shocks in brass vessel in air. Microphone inside. Vertical position with wedge-shaped cavity. 1 - first shock, 2 - second shock, etc.
B = volume of air bubble. E = energy released in blow.

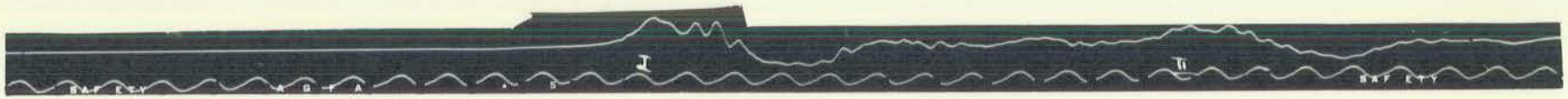

1) #28 3-9-42 B = 540 cu mm E = 11.7 x 10^6 ergs. x scale: 143 μsec/mm, y scale: 1.8 mlv/mm

2) #26 3-9-42 B = 317 cu mm E = 11.7 x 10^6 ergs. x scale: 189 μsec/mm, y scale: 1.9 mlv/mm

3) #19 3-9-42 B = 160 cu mm E = 11.7 x 10^6 ergs. x scale: 149 μsec/mm, y scale: 5.2 mlv/mm

4) #3 3-9-42 B = 87 cu mm E = 11.7 x 10^6 ergs. x scale: 156 μsec/mm, y scale: 33 mlv/mm

5) #7 3-9-42 B = 46 cu mm E = 11.7 x 10^6 ergs. x scale: 164 μsec/mm, y scale: 6.3 mlv/mm

PLATE 18A

6) #1 3-9-42 B = 25.6 cu mm E = 11.7 x 10^6 ergs. x scale: 123 μsec/mm,y scale: 31 mlv/mm

7) #9 3-9-42 B = 11.7 cu mm E = 11.7 x 10^6 ergs. x scale: 154 μsec/mm,y scale: 31 mlv/mm

8) #33 3-9-42 B = 4.2 cu mm E = 117 x 10^6 ergs. x scale: 84 μsec/mm,y scale: 28 mlv/mm

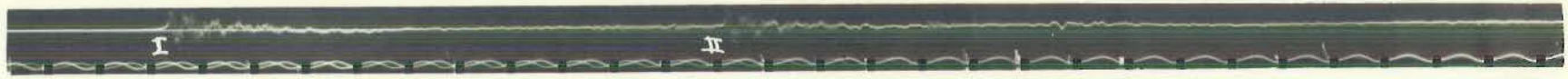

9) #16 3-9-42 B = 1.8 cu mm E = 11.7 x 10^6 ergs. x scale: 132 μsec/mm,y scale: 32 mlv/mm

PLATE 18B

Oscillograms of shocks in brass vessel in air. Microphone inside. Horizontal position with slab-shaped cavity. 1 - first shock, 2 - second shock, etc. B = volume of air bubble E = energy released in blow.

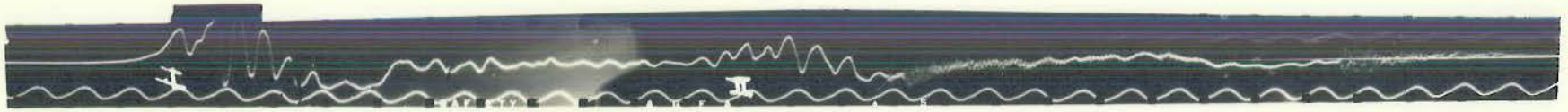

1) #32 3-9-42 B = 419 cu mm E = 117 x 10^6 ergs. x scale: 143 μsec/mm, y scale: 1.7 mlv/mm

2) #4 3-9-42 B = 140 cu mm E = 11.7 x 10^6 ergs. x scale: 161 μsec/mm, y scale: 32 mlv/mm

3) #23 3-9-42 B = 49.2 cu mm E = 11.7 x 10^6 ergs. x scale: 152 μsec/mm, y scale: 4.0 mlv/mm

4) #2 3-9-42 B = 23.6 cu mm E = 11.7 x 10^6 ergs. x scale: 140 μsec/mm, y scale: 28 mlv/mm

5) #6 3-9-42 B = 10.9 cu mm E = 11.7 x 10^6 ergs. x scale: 130 μsec/mm, y scale: 30 mlv/mm

PLATE 19A

6) #10 3-9-42 B = 6.4 cu mm E = 11.7 x 10^6 ergs. x scale: 167 μsecs/mm, y scale: 24 mlv/mm

7) #21 3-9-42 B = 3.15 cu mm E = 11.7 x 10^6 ergs. x scale: 148 μsec/mm, y scale: 33 mlv/mm

PLATE 19B

DECLASSIFIED

Oscillograms of shocks in brass vessel in water. Microphone inside and outside (Nos. 8, 11, 12 and 13). Vertical position. 1 - first shock, 2 - second shock, etc.
B = volume of air bubble. E = energy released in blow.

1) #6 1-3-42 B = 389 cu mm E = 13.6×10^6 ergs x scale: 154 μsec/mm, y scale: 4.6 mlv/mm

2) #7 1-3-42 B = 240 cu mm E = 13.6×10^6 ergs x scale: 122 μsec/mm, y scale: 5.8 mlv/mm

3) #10 1-3-42 B = 80 cu mm E = 13.7×10^6 ergs x scale: 65 μsec/mm, y scale: 10 mlv/mm

4) #10 1-6-42 B = 30.6 cu mm E = 5.13×10^6 ergs x scale: 137 μsec/mm, y scale: 2.6 mlv/mm

5) #10 12-26-41 B = 11.1 cu mm E = 8.1×10^6 ergs x scale: 52 μsec/mm, y scale: 28 mlv/mm

PLATE 20A

6) #7 12-26-41 B = 7.65 cu mm E = 12.7 x 10^6 ergs x scale: 58 μsec/mm,y scale: 27 mlv/mm

7) # 1 12-29-41 B = 1.01 cu mm E = 12.5 x 10^6 ergs x scale: 68 μsec/mm,y scale: 34 mlv/mm

8) #3 12-29-41 B = 0.60 cu mm E = 12.5 x 10^6 ergs x scale: 63 μsec/mm,y scale: 47 mlv/mm

9) #4 12-29-41 B = 0.32 cu mm E = 9.0 x 10^6 ergs x scale: 68 μsec/mm,y scale: 32 mlv/mm

10) #4 12-23-41 B = 0.113 cu mm E = 6.4 x 10^6 ergs x scale: 60 μsec/mm,y scale: 22 mlv/mm

11) #5 12-22-41 B = 0.065 cu mm E = 6-5 x 10^6 ergs x scale: 72 μsec/mm,y scale: 26 mlv/mm

PLATE 20B

12) #11 12-23-41 B = 0.034 cu mm E = 7.65×10^6 ergs x scale: 72 μsec/mm, y scale: 29 mlv/mm

13) #2 12-19-41 B = 0.004 cu mm E = 13.4×10^6 ergs x scale: 81 μsec/mm, y scale: 38 mlv/mm

PLATE 20C